Room-temperature compound semiconductor radiation detectors

D.S. McGregor[a,*], H. Hermon[b]

[a]*Nuclear Engineering Department, The University of Michigan, Ann Arbor, MI 48109-2104, USA*
[b]*Sandia National Laboratories, MS-9671, Livermore, CA 94551, USA*

Abstract

A summary is presented of the present status of several compound semiconductor radiation detectors, including detectors fabricated from GaAs, HgI_2, CdTe, $Cd_{1-x}Zn_xTe$ and PbI_2.

1. Introduction

In 1945, Van Heerden successfully fabricated solid-state radiation conductivity counters, in which he describes the detection of alpha particles and gamma rays with AgCl crystals in his thesis "The Crystal Counter" [1]. The exciting results of Van Heerden's work gave rise to an entirely new class of radiation detector, now commonly referred to as semiconductor detectors. Two of the first extensive reviews on semiconductor detectors (or "crystal conductivity counters") were presented in 1949 by Hofstadter [2,3] and in 1952 by Chynoweth [4]. The fundamental operation of the devices is described, as well as familiar difficulties such as space-charge fields and charge carrier trapping. Due to the difficult problems imposed on the operation of semiconductor detectors by charge carrier trapping and space-charge accumulation, semiconductor detectors were viewed with some skepticism, in which it was thought that they would offer little advantage over scintillation detectors [4,5]. The great success of high-purity Ge and Si radiation spectrometers overcame the skepticism [6], yet charge carrier trapping, space-charge accumulation and polarization are indeed still significant issues for compound semiconductors. Nevertheless, the unique material properties of several compound semiconductors render them attractive in radiation detector applications for situations where Ge and Si are unsuitable.

Room-temperature operation, for instance, requires that the semiconductor band gap energy be appropriately large to reduce thermally generated leakage currents. High-resolution radiation spectroscopy requires a small band gap energy to ensure a low average ionization energy (ε), hence increasing the number of charge carriers excited for specific ionizing radiation energies while reducing resolution degradation from statistical fluctuations [7]. Photoelectric interactions in the detecting material are preferred for gamma ray spectroscopy; hence, compound semiconductors for efficient gamma ray spectroscopy should be composed of high Z materials [7,8]. Additionally, high gamma ray interaction efficiency demands that high-quality material be available in large volume. Charged particle detectors for use in a high gamma ray environment are best composed of low Z materials in order to reduce background gamma ray interactions. High carrier mobilities and long carrier mean free drift times (τ^*) are advantageous for high-resolution radiation spectroscopy [9–12], although short carrier mean free drift times are often desired for high-speed timing measurements [13]. High charge carrier mobility is desirable for situations requiring low detector operating voltages and short electronic shaping times. Ultimately, a semiconductor should be chosen according to the material and electrical properties that best match the particular radiation measurement to be performed.

The compound semiconductors generally of interest for room-temperature operation have band gap energies between 1.35 and 2.55 eV [14–17], although not all of these compound semiconductors are readily available due to either growth difficulties, handling issues or economics. Several compound semiconductors that have obvious advantages for specific applications are simply not available. As a result, the most generally promising and available materials receive much more attention than many other interesting compound semiconductors. A comparison of the properties of several compound semiconductor materials and detectors is presented in Table 1. Fig. 1 illustrates a few compound semiconductors at various stages of detector fabrication. Presently,

* Corresponding author. Tel. + 1 313 647 8964; fax + 1 313 647 8964; e-mail: dsmcgreg@umich.edu.

Table 1
Properties of semiconductor detectors and materials

Material	Crystal structure	Atomic number Z	Density g/cm³	Operating temp. (K)	Band gap (eV)	Energy per e/h pair (eV)	Drift mobility (cm²/V s) electron	Drift mobility hole	Mean free drift time (s) electron	Mean free drift time hole	Typical detector thickness	5.9	60	122	356	662	FWHM (keV) α-particles 5.5 MeV
Ge	Cubic	32	5.33	77	0.72	2.98	36000	42000	$>10^{-4}$	$>10^{-4}$	Up to 10 cm	0.114	0.3	0.4		0.9	13
Si	Cubic	12	2.33	295	1.12	3.6	1450	450	$>10^{-4}$	$>10^{-4}$	Up to 2.5 cm	0.255	0.4	0.55		0.9	
GaAs epitaxial	Cubic (ZB)	31/33	5.32	295	1.424	4.3	>8000	400			50–200 μm		2.5	2.6			20–24
bulk				295						4×10^{-5}	100–500 μm		8.05	8.83	17.8		60–150
PbI₂	Hexagonal	82/53	6.2	295	2.55	4.9	8	2	10^{-6}	3×10^{-7}	100 μm	0.5	1.83				
HgI₂	Tetragonal	80/53	6.4	295	2.13	4.3	100	4	7×10^{-6}	3×10^{-6}	0.2–3.0 mm	0.2	0.9–1.8	3.2	6.4	5.96–15.9	
CdTe	Cubic (ZB)	48/52	6.06	295	1.52	4.43	1000	80	10^{-6}	10^{-6}	0.1–5.0 mm	1.1	1.7	5.0	6.4	5.7	
Cd₀.₈Zn₀.₂Te	Cubic (ZB)	48/30/52	≈6	295	1.6	5.0	1350	120	10^{-6}	2×10^{-7}	1–10 mm		2.5	3.35	6.46	11.8–16.1	
InP	Cubic (ZB)	49/15	4.79	295	1.35	4.2	4600	150	–	–	25–500 μm						275
CdSe	Hexagonal	48/34	5.8	295	1.73	–	720	75	–	–	0.2 1.0 mm	1.4	8.5				
GaSe	Hexagonal	31/34	4.55	295	2.03	4–45	60	215	–	–	50–150 μm						220

the compound semiconductors receiving most attention for radiation detector applications are GaAs, HgI₂, CdTe and most recently $Cd_{1-x}Zn_xTe$. In the following sections, developments in the progress of compound semiconductor radiation detectors, in the past and more recently, are described in more detail.

2. Generating operation

The operating environment and type of radiation a device is to detect predetermines the semiconductor that should be utilized. Gamma ray energy absorption through the photoelectric process is strongly dependent on the atomic number of the detector material, since the photoelectric absorption coefficient is proportional to Z^{4-5} [7]. As a result, it is generally the atomic density of the highest atomic number element in the material that determines the gamma ray absorption efficiency, not the average atomic number of the material. For instance, InP and GaAs both have an average atomic number of 32; however, gamma ray photoelectric absorption in InP is higher than in GaAs since the atomic number of In (49) is much higher than that of Ga (31) or As (33). Since the photoelectric effect is preferred over Compton scattering as a mechanism for absorbing gamma ray energy, materials with high Z numbers are preferred for gamma ray detection. In a very different case, in which energetic charged particles are to be measured in a high gamma ray environment, low Z materials (such as silicon) may be preferred in order to reduce background noise from gamma ray interactions. In some circumstances, low atomic number semiconductor materials may be preferred for beta particle measurements since backscattering is lower for low Z materials than that of relatively high Z materials.

The leakage current of a semiconductor radiation detector is primarily determined by the band gap energy of the material and the device structure. The intrinsic carrier concentration for a semiconductor is proportional to $e^{-(E_g/kT)}$ where E_g is the energy of the band gap, k is Boltzmann's constant and T is the absolute temperature [18]. Semiconductors with small band gap energies, (such as Ge), must be cooled to reduce the carrier concentrations to acceptably low noise levels. Semiconductors with relatively large band gap energies can often be operated at room temperature and, in some cases, at elevated temperatures. However, a material that has a wide band gap may still have a relatively high free carrier concentration if the material is contaminated with a high concentration of electrically active impurities. Generally, detectors manufactured from materials with low to moderate band gap energies (1.12–1.45 eV) are fabricated with rectifying contacts to reduce leakage current. Semiconductor materials can also be developed with deep energy levels in the material to compensate
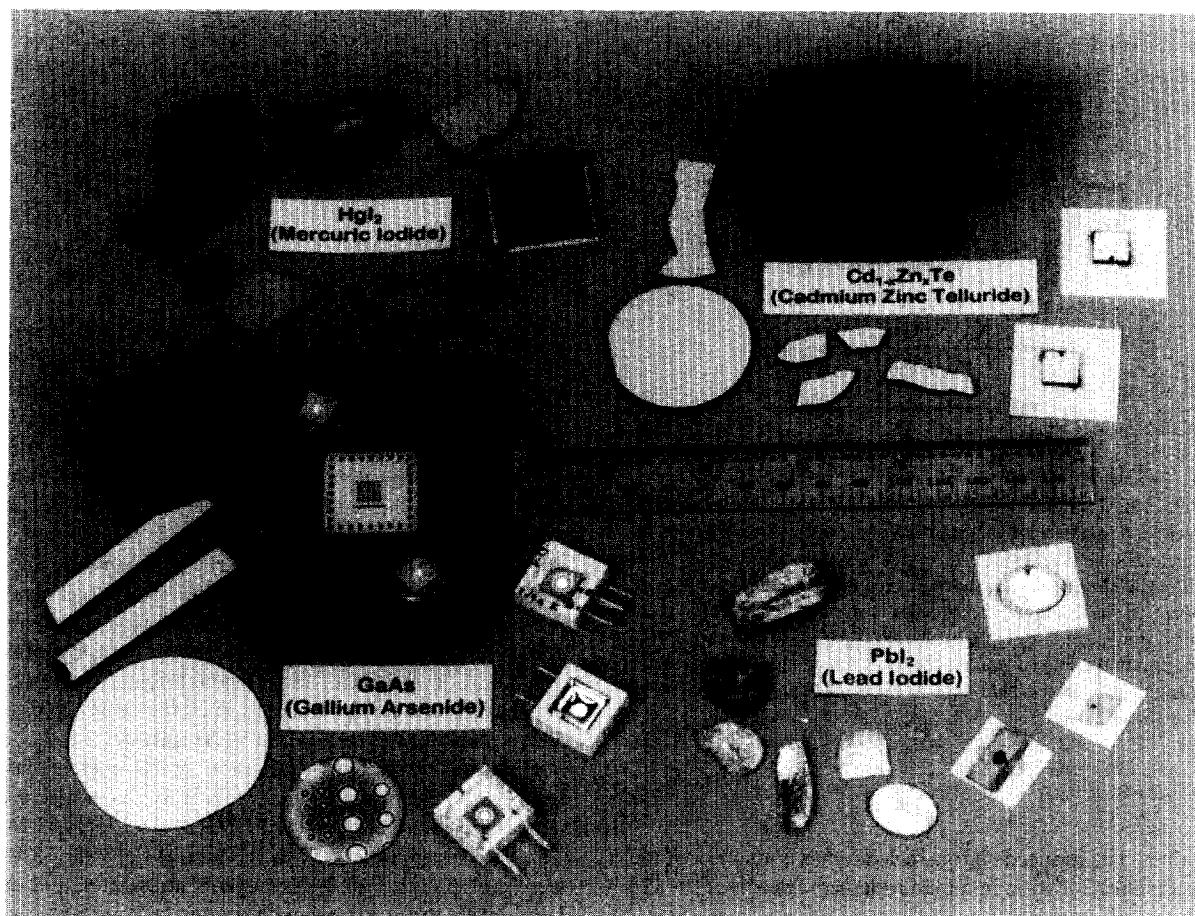
Fig. 1. An assortment of compound semiconductor materials at various stages of detector processing and fabrication. Shown are samples of HgI$_2$, CdZnTe, GaAs and PbI$_2$.

shallow impurity levels, thereby producing very high resistivity material. Unfortunately, the introduction of deep or shallow energy levels into a semiconductor can have adverse effects on the charge carrier mean free drift times and the internal electric field.

A planar semiconductor detector is operated by applying a voltage across contacts on opposite sides of the device. Ionizing radiation (for instance, gamma rays or charged particles) absorbed in the material excites electron–hole pairs in proportion to the energy deposited in the detector (Fig. 2). These free charges then drift through the applied electric field, creating an induced charge at the terminals of the device proportional to the distance traveled by the charge carriers (both electrons and holes) through the applied electric field. It is this induced charge that is measured to determine the energy of the absorbed radiation. The general relationship for the change in induced charge at the detector contacts is described by the Shockley–Ramo theorem [19,20], in which

$$dQ^* = \frac{qN_0}{W} dx, \tag{1}$$

where Q^* is the induced charged, N_0 is the initial number of electron–hole pairs, and W is the detector width. In a detector fabricated from very pure, trap-free semiconductor material, full charge carrier collection at the electrodes is possible and the total induced charge is simply $Q^* = qN_0$. Unfortunately, this is generally not the case with most compound semiconductors, and the effect of charge carrier loss from trapping must be taken into account. Hecht's relation [21] describes the effect of charge carrier transport in a uniform field, assuming that the charge carrier velocities and the mean free drift lengths of the charge carriers can be defined by single
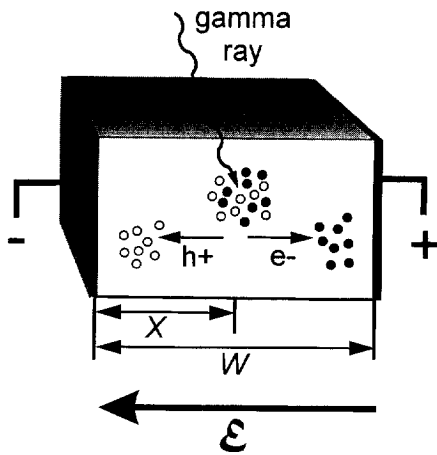
IV. DETECTOR MATERIALS

Fig. 2. Basic planar detector operation, in which charge carriers excited at location *x* by a quantum of radiation are separated by an electric field and swept to opposite contacts of the device. If all of the charge carriers, both electrons (e-) and holes (h +), are swept to the contacts, the process is referred to as "full charge collection". Yet, the signal measured is from the induced charge produced by the motion of the charge carriers as they move through the electric field, and not the charge of the "collected" electrons and holes.

values. The induced charge measured as a function of the interaction location in a planar detector becomes [9–12]

$$Q^* = qN_0 \left[\frac{v_h \tau_h^*}{W} \left(1 - \exp\left[\frac{-x}{v_h \tau_h^*} \right] \right) \right.$$
$$\left. + \frac{v_e \tau_e^*}{W} \left(1 - \exp\left[\frac{(x - W)}{v_e \tau_e^*} \right] \right) \right], \tag{2}$$

where v is the charge carrier velocity, τ^* is the charge carrier mean free drift time, x represents the location between the parallel contacts of the initial radiation interaction, and the e and h subscripts refer to electrons and holes, respectively. The induced charge for a single event is then dependent on the interaction position and the ratio $v\tau^*/W$ (referred to elsewhere as the carrier extraction factor [12]), and the resulting energy resolution can be significantly degraded if one (or both) of the charge carrier mean free drift times (electrons or holes) is relatively short [9–12]. The induced charge varies with detector shape and contact geometry [10,19,22] and alternative detector configurations to the simple planar design can help to improve detector energy resolution [7,23]. Electronic noise contributions [24,25] and series resistance [26–29] can also play a major part in reducing detector spectroscopic performance. Statistical fluctuations in the number of charge carriers excited per ionizing event ultimately limits the highest achievable energy

resolution, as described by [7]

$$R_{FWHM} = 2\sqrt{2\ln(2)\varepsilon EF}, \tag{3}$$

where R_{FWHM} is the FWHM energy resolution, ε is the average ionization energy, E is the gamma ray energy, and F is the Fano factor [30].

3. GaAs detectors

Gallium arsenide (GaAs) has been studied as a radiation detector material since the early 1960s [31,32] and was the first compound semiconductor to demonstrate high resolution for gamma rays at room temperature (RT) [33–41]. Material development for GaAs radiation detectors has been slow, although there has been a surge of interest over the last few years [42]. GaAs has a cubic, zincblende crystal structure with atomic numbers of 31 and 33, hence the relative gamma ray photoelectric interaction probability is similar to Ge. GaAs has many promising features, including a moderately wide band gap (1.424 eV) and relatively high charge carrier mobilities. Additionally, GaAs device and fabrication technologies have matured significantly since the early 1960s as a direct result of efforts in the VLSI industry.

High-resolution GaAs radiation spectrometers have been fabricated primarily from relatively thick, high-purity, liquid-phase epitaxial (LPE) GaAs [35,36,38,43,44]. The LPE layers described in the literature [35,36,38,43] were grown on n-type low resistivity substrates, and the LPE layers were n-type with impurity concentrations ranging between $6 \times 10^{12}/cm^3$ and $2 \times 10^{14}/cm^3$. In all cases, the detector structures utilized evaporated Au or Pd Schottky barrier blocking contacts, between 1.5 and 3 mm in diameter, to reduce leakage current. The n-type substrates were contacted by either evaporated Al or a low resistance Ga–In eutectic alloyed to the substrate. Schottky barrier GaAs LPE detectors have demonstrated RT resolution of 20–24 keV FWHM for 5.5 MeV alpha particles [35,36,38]. Detectors tested by Eberhardt et al. [33–35] were between 60 and 80 µm thick with energy resolution at 22°C of 2.6 keV FHWM for 122 keV gamma rays. Similar results were reported by Gibbons and Howes [38] and Kobayashi et al. [36]. More recently, 200 µm thick LPE detectors have been prepared by Alexiev and Butcher [43] with RT energy resolution of 2.35 for 59.5 keV gamma rays. An alternative structure reported by Lauter et al. [45] utilizes a molecular beam epitaxially (MBE) grown p-Al-GaAs/GaAs staircase multiplier structure coupled to a 4.5 µm thick MBE-grown GaAs absorption region. While the thin device design ultimately compromises gamma ray interaction efficiency, the device demonstrated RT energy resolution of 1.4 keV FWHM for 17.8 keV gamma rays.

Overall, recent LPE GaAs gamma ray detectors have increased in thickness while retaining high-energy resolution at room temperature, thus demonstrating their potential for room temperature X-ray and low-energy gamma ray spectrometers. Epitaxial GaAs detectors remain primarily experimental, however, in that the devices are difficult to reproduce and are still relatively small in volume, resulting in expensive detectors with low gamma ray interaction efficiency. Commercial application of epitaxial GaAs high-resolution X-ray and low-energy gamma ray spectrometers can become a reality when improved epitaxial growth methods are realized that increase both surface area and thickness while retaining the high material quality characteristic of LPE growth at a reduced cost.

Such stringent demands on GaAs epitaxial growth have led many researchers to investigate bulk-grown, semi-insulating (SI) GaAs as a room-temperature radiation detector [42]. Undoped SI bulk GaAs is compensated through a careful balance between native deep-level donors (denoted EL2 [46]) and shallow acceptor and donor impurities [47,48]. The resistivity of compensated SI bulk GaAs, generally between 10^7 and 10^8 Ω cm, is still not high enough to reduce the leakage current for high-resolution RT spectroscopy. To reduce the leakage current, diode detector designs are often employed, in which the basic device structures generally consist of a blocking contact and a low resistivity contact (often referred to as an "ohmic contact") on opposite sides of a GaAs substrate. On bulk SI GaAs material, the blocking contact is generally a Schottky barrier, a diffused p-type barrier, or an epitaxially grown p-type barrier. Device construction has matured to the extent that Schottky barrier blocking contacts are fabricated with room-temperature leakage current densities less than 10 nA/mm² during high-voltage operation [49]. Doped p-type AlGaAs blocking barrier detectors demonstrate potentially lower leakage current densities than Schottky barrier detectors [49]. Under reverse bias, the electric field in undoped SI bulk GaAs diode detectors is separated into high and low field regions, where the high field region is adjacent to the blocking Schottky contact [32,42,50–55]. Numerous experimental techniques have been employed over the past few years to measure the dependence of the unique high field region as a function of bias voltage. These include charged particle probing [50,53], optical transmission [51,52], optical excitation [32,55], electron beam excitation [54] and direct contact probing [51,52]. The general indication is that the high field region is fairly constant in magnitude (flat field), indicating relatively low net space charge, and the active region width increases as a linear function of applied reverse bias voltage, requiring 1–2 V per micron of thickness of the active region. There is some indication that the electron capture cross section of the EL2 deep donor increases with increasing electric field [56–58], and models taking this phenomenon into account [53,59–61]

simulate the observed electric field distribution [32,51,52]. In general, space-charge contributions from the compensating deep levels are thought to be the cause of the unusual active region dependence, and several models have been proposed which take the role of the EL2 deep donor defect charge state into account [50,53,59–63].

The performance of bulk GaAs gamma ray and charged particle spectrometers has consistently improved over the past few years, primarily due to improvements with both bulk GaAs material properties and detector fabrication processes. Schottky barrier detectors fabricated from SI bulk GaAs routinely demonstrate RT energy resolution of 140 keV FWHM or lower for 5.5 MeV alpha particles [53,64,65]. Reduced temperature ($-10°$C) energy resolution for a 300 μm thick bulk GaAs detector, reported by Holland et al. [66], is 9.2 keV FWHM for 122 keV gamma rays, and reduced temperature ($-30°$C) energy resolution for a 100 μm micron thick bulk GaAs detector reported by Bertuccio et al. [67] is 2.1 keV FWHM for 60 keV gamma rays. Doped p-type barrier and p-AlGaAs barrier detectors 400 μm thick have demonstrated RT energy resolution between 16.5 and 21.5 keV FWHM for 122 keV gamma rays [49,51]. Small area (0.5 mm²) bulk GaAs devices have demonstrated relatively good energy resolution at RT for 130 μm thick devices [49]. The best device demonstrated RT energy resolution of 8.05 keV FWHM for 60 keV gamma rays and 8.83 keV FWHM for 122 keV gamma rays (Fig. 3).

Ultimately, high-quality epitaxial GaAs gamma ray spectrometers are limited by available material volume, and the performance of bulk GaAs radiation spectrometers is limited by short carrier mean free drift times. The charge collection efficiency for SI bulk GaAs was observed to improve as resistivity (and presumably deep donor EL2⁻ concentrations) decreased [68]. Attempts to reduce deep-level traps and impurity concentrations in bulk GaAs through zone refining and zone leveling have thus far failed to produce radiation spectrometers of reasonable quality [49]. Nevertheless, other applications for bulk GaAs radiation detection devices have been reported, including particle detection for high-energy physics [69–74], radiation dose monitoring through nuclear displacement [75], pixel arrays for X-ray imaging [76], pixel arrays for thermal neutron imaging [77] and high-speed radiation pulse detection [78–84].

4. HgI₂ detectors

Mercuric iodide (HgI₂) has been investigated as a room-temperature gamma ray detector since the early 1970s [85–92]. HgI₂ has atomic numbers of 80 and 53, with a volume density of 6.4 g/cm³. HgI₂ (α-phase) has recorded charge carrier mobilities of 4 cm²/V s for holes and 100 cm²/V s for electrons [92], thus a substantial
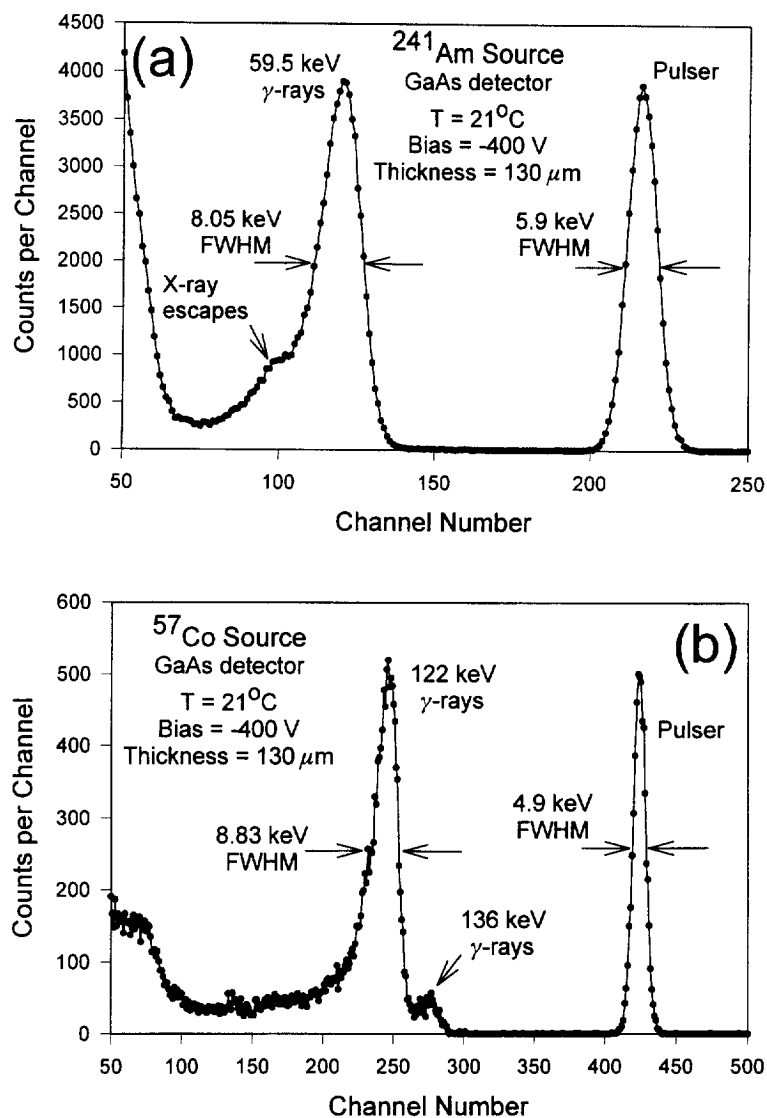
Fig. 3. Room temperature gamma ray spectra (21°C) taken with a 130 μm thick bulk SI GaAs radiation detector. The detector area is 0.5 mm², and the operating voltage is 400 volts. Shown are spectra from (a) 59.5 keV ²⁴¹Am gamma rays and (b) 122 keV ⁵⁷Co gamma rays.

voltage is generally required to ensure acceptably high charge carrier collection. HgI_2 has a measured average ionization energy of 4.42 eV/e–h pair, and a measured Fano factor of 0.19 [93]. Due to the large atomic number of Hg (80), the photoelectric effect is the predominant means by which gamma rays interact in HgI_2 for energies up to 400 keV [87]. HgI_2 detectors can be relatively smaller than Ge, GaAs, CdTe or CdZnTe detectors for a required gamma ray efficiency. For instance, 2 mm thick HgI_2 detectors will have a photoelectric absorption efficiency for 140 keV gamma rays comparable with

4.2 mm thick CdTe or CdZnTe detectors and 1.9 cm thick Ge or GaAs detectors.

HgI_2 forms in a tetragonal lattice at temperatures below 130°C, appearing red in color (α phase) with a band gap energy of 2.13 eV [94,95]. Red HgI_2 is a layered crystal with cleavage planes parallel to the (0 0 1) planes. At temperatures above 130°C, HgI_2 undergoes a phase transformation to an orthorhombic lattice (β-phase), appearing yellow in color with a band gap of 2.5 eV. Red HgI_2 will change to the β-phase when heated above 130°C, and will change destructively back to the

α-phase when cooled below 130°C. As a result, HgI$_2$ detectors are usually operated in environments that allow the crystal temperature to remain well below 130°C.

HgI$_2$ solution growth was the first method to produce HgI$_2$ crystals for detectors, and solution-grown devices have demonstrated some gamma ray spectroscopic performance [96–98]. The crystals were seeded from a single crystal of α-HgI$_2$ in which the large HgI$_2$ crystal was grown from a solution of DMSO/MeOH (dimethylsulfoxide/methanol) or DMSO/EA (dimethylsulfoxide/ethyl acetate) saturated with HgI$_2$ and maintained at a temperature between 25°C and 40°C, as described by Nicolau and Joly [96]. The resulting material was optically clear and had relatively low dislocation densities. Radiation detectors (0.5 mm thick) fabricated from the solution grown material demonstrated RT gamma ray energy resolution of 2.3 keV FWHM for 59.5 keV gamma rays and 6 keV FWHM for 122 keV gamma rays.

Due to impurity and solvent inclusions commonly found with solution grown HgI$_2$, vapor-phase processes remain the preferred growth method for HgI$_2$. Two distinct methods of vapor growth are the vertical ampoule method and the horizontal method. The vertical method uses an arrangement similar to the temperature oscillation method originally developed by Scholz [99], and the method allows the growth of large HgI$_2$ crystals [100–103]. Briefly described, HgI$_2$ that has been vapor purified [104] is vacuum sealed into an ampoule. The HgI$_2$ material is first heated so that it accumulates at the top of the ampoule. A cold finger is brought into close contact with the ampoule base pedestal, thus providing the required temperature gradient for nucleation and growth. There are three main thermal elements to control: the cold finger, the base heating element and the axial heating element. Once a perfect single crystal is nucleated at the pedestal, the temperature gradient between the source and the seed is kept high enough to sustain a constant rate of growth. A seed crystal is generally not used for the growth process. High-quality HgI$_2$ single crystals between 250 g and 1 kg can be produced within several weeks. Figs. 4 and 5 show a typical arrangement for vertical ampoule vapor-phase growth of HgI$_2$.

Horizontal vapor-phase growth is performed by inserting a vacuum-sealed ampoule with purified HgI$_2$ into a horizontal furnace [100,105–107]. There are two basic horizontal growth methods: horizontal growth for the formation of a single crystal in an ampoule [101], and horizontal platelet growth in which multiple crystals are formed. In platelet growth, a temperature gradient is sustained along the length of the ampoule such that numerous small HgI$_2$ platelets grow in an optimum growth location. The horizontal method provides a means to rapidly produce numerous, but small, spectrometer-grade HgI$_2$ crystals. HgI$_2$ crystals grown in the
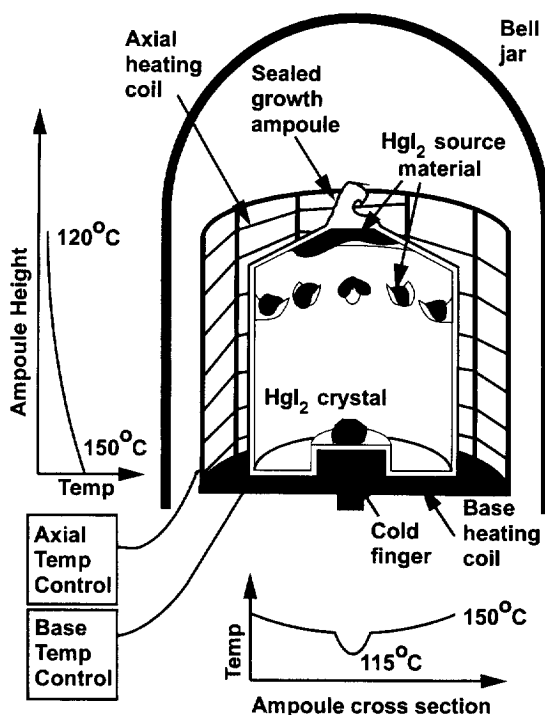

Fig. 4. Schematic drawing of a vapor-phase vertical crystal growth ampoule and heater arrangement used for the growth of bulk HgI$_2$.

microgravity environment of space demonstrated electrical characteristics superior to ground-based growth samples [108–110]. The improvements are believed to be partially due to the absence of convection currents (which also permitted an increased growth rate), and the absence of gravitational influence on crystal slip planes.

HgI$_2$ detectors are generally prepared from bulk crystals by cleaving samples perpendicular to the c-axis. A thin blade is often used to separate crystal planes; however, much skill and care must be exercised to produce the high-quality surfaces necessary for good spectrometer performance. String sawing with a 25% KI in water-etch solution and abrasive slurry wire cutting are also used [111]. Chemical lapping is performed primarily with 20% KI in water solution on felt lapping wheels. Samples are generally etched in a KI solution before contacts are applied. HgI$_2$ is a soft crystal that reacts with numerous metals, hence detector contact material selection is limited. Presently, the most commonly used contact materials are colloidal carbon (Aquadag) and Pd. Thermal evaporation of Pd allows for simple electrode patterning; however, substantial sublimation of the HgI$_2$ can occur in the evacuated environment, especially during radiant heating by the molten source, if proper
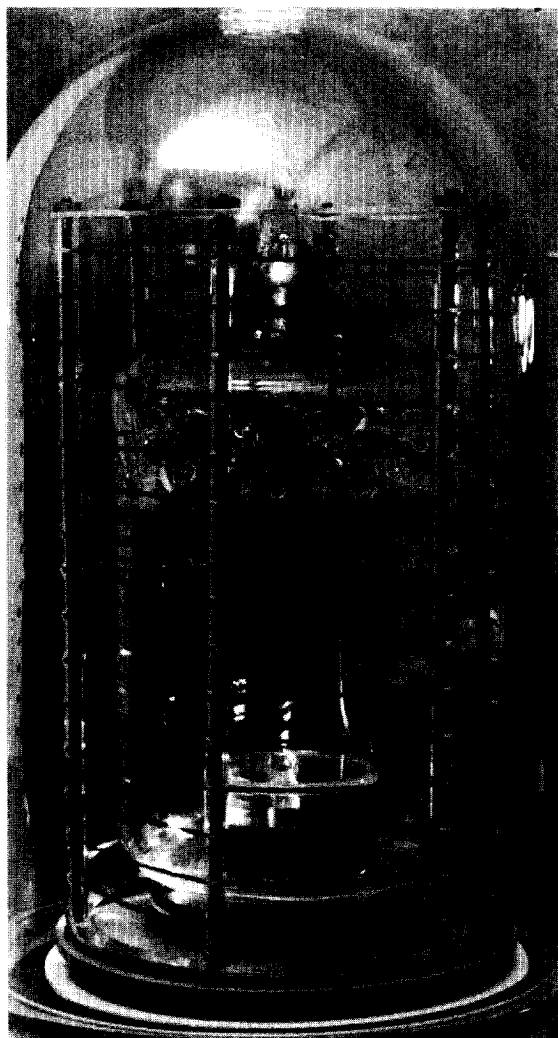
Fig. 5. Photograph of bulk HgI_2 being grown by vapor-phase transport in a vertical crystal growth ampoule.

precautions are not taken. The detectors are connected to supporting electronics with Pt wires. The exposed surfaces of HgI_2 detectors also tend to decompose over time, a process that can be substantially retarded to negligible levels by encapsulating the finished detectors in parylene.

Charge carrier trapping and space-charge polarization have long been issues with HgI_2 radiation detectors [112–119]. Polarization, an effect that causes a progressive change in observed pulse height with time, is believed to be the result of accumulating space charge in the material. Native defects and space charge, impurity diffusion (or drift), processing damage and contamination (or a combination of all of these) have some influence on polarization effects. Devices often perform best after

a voltage bias has been applied for a considerable period of time [117], and the gamma-ray energy resolution improves dramatically over a period of several days. The problem of polarization has reportedly been reduced through improved material processing and encapsulation techniques [112].

Planar detectors fabricated from large, bulk-grown HgI_2 crystals have demonstrated room temperature gamma-ray energy resolution below 16 keV FWHM at 662 keV for devices up to 2.2 mm thick with contact areas up to 3.5 cm^2 [120,121]. Small planar devices fabricated from small platelet-grown HgI_2 also have very high room temperature energy resolution. The electronic and thermal noise of small HgI_2 devices are low enough that the detectors can be used for low-energy gamma-ray and X-ray fluorescence spectroscopy [122]. Fig. 6 shows a room-temperature ^{241}Am gamma-ray spectrum taken with a 700 μm thick HgI_2 detector, with a measured RT energy resolution of 1.9 keV FWHM for 59.5 keV gamma rays. Thick planar devices are affected by position-dependent charge collection and resolution degrades as a result, but alternative detector designs have shown improved results. The spectroscopic performance of circular drift detectors and coplanar detectors have been compared. While both have demonstrated improved resolution over simple planar designs, a drift detector composed of concentric electrode rings demonstrated better energy resolution than the coplanar design. Reported room-temperature energy resolutions were 3.2 keV FWHM for 122 keV gamma rays and 5.96 keV FWHM for 662 keV gamma rays [123]. Fast neutron irradiation tests performed on a few HgI_2 detectors indicated that the material demonstrated only minor changes in resolution at fluences up to 10^{15} n/cm^2 [124]. However, the resolution was poor to begin with for charged particles, with reported resolutions between 5% and 20% FWHM for various proton and alpha particle energies, and activation became apparent with the observation of increased gamma ray background.

CsI(Tl) is an attractive scintillation material with a higher light output than NaI(Tl); unfortunately, the response of typical bialkali photomultiplier tubes does not match well the emission spectrum of CsI(Tl). HgI_2 photodetectors have very high photocurrent response for photons with wavelengths near 585 nm, which matches well to the peak emission spectrum of CsI(Tl) [125–128], and HgI_2 detectors have been demonstrated as viable detectors for compact scintillator radiation detection systems [125,126,128–135]. The electrodes on the detectors must be transparent for best performance, and the choice of transparent electrodes has been shown to affect the observed quantum efficiency of the HgI_2 device [131]. Markakis [129] reports a RT energy resolution of 33 keV FWHM for 663 keV gamma rays with a 1 in. diameter × 1 in. thick CsI(Tl) scintillator coupled to a 1 in. diameter × 2 mm thick HgI_2 detector (see Fig. 7).
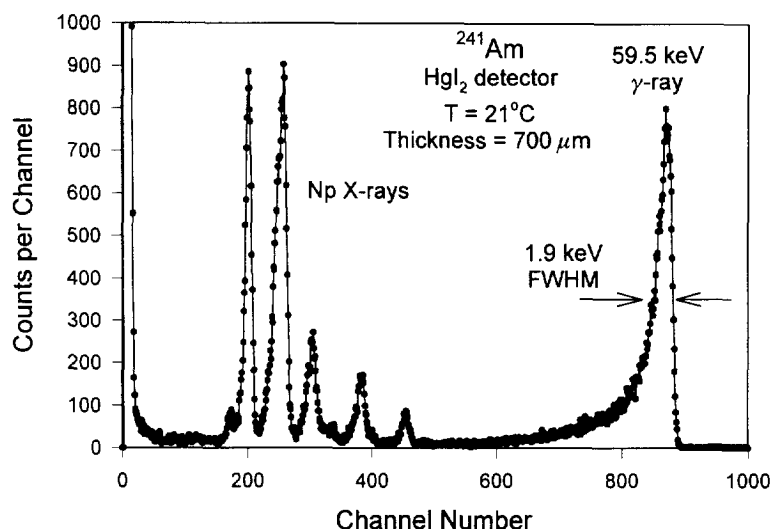
Fig. 6. Room-temperature (21°C) spectrum of ^{241}Am gamma rays taken with a platelet grown 700 μm thick HgI$_2$ detector. The devices are utilized in commercially available, portable X-ray fluorescence analysis field instruments.
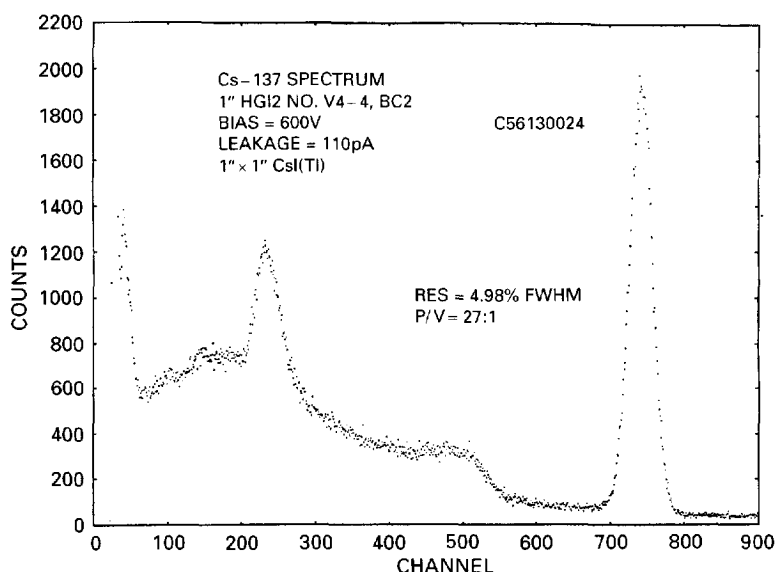
Fig. 7. ^{137}Cs spectrum obtained using a 1 in. diameter × 2 mm thick HgI$_2$ photodetector coupled with a 1 in. diameter × 1 in. thick CsI(Tl) scintillator (from J.M. Markakis [129]).

Other CsI(Tl)/HgI$_2$ devices have attained similar resolutions [130–135]; Wang [132] reports a RT energy resolution of 42.6 keV FWHM for 1.332 MeV gamma rays with a 0.5 in. diameter HgI$_2$ detector coupled to a 0.5 in. diameter × 0.5 in. thick CsI(Tl) scintillator.

HgI$_2$ detectors have been used for various room temperature applications, including X-ray and gamma ray imaging [136–144], medical instrumentation [145–147], X-ray astronomy and space applications [148–151], energetic neutron recoil detection [152], Pu monitoring [153], and X-ray fluorescence spectroscopy [154]. HgI$_2$ detectors are commercially available, as well as several instruments that utilize HgI$_2$ detectors for radiation sensing and spectroscopy.

IV. DETECTOR MATERIALS

5. CdTe detectors

Cadmium telluride (CdTe) has been investigated as a room-temperature gamma-ray detector since the mid-1960s [155–159], and various detailed review articles cover CdTe material and detector performance [23, 160–165]. CdTe has a cubic, zincblende crystal structure with atomic numbers of 48 and 52, and a volume density of 6.06 g/cm^3 [160]. Charge carrier mobilities are 80 cm^2/V s for holes and 1000 cm^2/V s for electrons, and the average ionization energy is 4.43 eV/e–h pair [23]. Photoelectric absorption is the dominant gamma-ray interaction mechanism in CdTe for energies up to approximately 260 keV [87].

Details of CdTe crystal growth, using a number of different methods [161–171], are described extensively in the literature [162–164]. Vertical zone melt growth of CdTe ingots has yielded relatively large single crystals (see Ref. [163]), and recent results by Chang et al. indicate that fairly high resistivity ingots with low-etch pit densities can be grown [171]. Variations of Bridgman growth produced large ingots of CdTe (see Ref. [163,164]); however the material is generally less suitable for gamma-ray spectrometers due to background impurity inclusions during the growth process. Indium doped, vertical Bridgman grown CdTe material has shown a RT energy resolution 43 keV FWHM for 662 keV gamma rays [172] for small devices. The traveling heater method (THM) is more commonly used for growing detector grade CdTe for several reasons including lower growth temperatures, reduced impurity concentrations, and lower defect concentrations than Bridgman techniques [164,165]. THM CdTe material is usually Cl doped to compensate background impurities and native defect states, thus increasing the material resistivity [166,167, 173–177]. Although good spectroscopic resolution can be observed from detectors fabricated with CdTe:Cl material, trapping and non-uniformities in the electrical properties of THM CdTe:Cl material generally restrict detector dimensions to relatively small sizes.

CdTe detectors are generally fabricated by first slicing and lapping samples to appropriate dimensions. Final alumina lapping abrasive particle sizes range between 0.1 and 0.3 µm [178–181]. The surfaces can be polished chemomechanically with a bromine/methanol solution, in which there is some indication that the etch rate is linear with respect to the bromine concentration [180]. Riedinger et al. [180] report that the best chemomechanical polishing results are achieved when the etchant products are effectively removed from the surface, which is apparently achieved with low bromine concentrations and relatively high polishing speeds. Although several etchants have been documented [164], samples are usually etched with a bromine/methanol solution before contacts are applied [164,178,179], usually ranging anywhere between 2% and 5% bromine

solution. Kohiki et al. [181] describe a process to improve the cleanliness of bromine/methanol etched CdTe surfaces, in which oxygen and argon bombardment of the surface is followed by thermal treatments.

Good ohmic contact formation on CdTe is generally performed with electroless deposition, in which noble metal salt solutions of AuCl$_3$, AgNO$_3$, and PtCl$_4$ have been used [161,162,164]. Apparently, the electroless noble metal salt solution etches the CdTe surface, and this is immediately followed by the redeposition of several layers in which both Cl and the noble metals are present [164]. Auger studies conducted by Hage-Ali and Siffert on CdTe [164] and by the authors on CdZnTe have shown that Cl incorporation can reach beyond 0.5 µm into the surface after PtCl$_4$ or AuCl$_3$ deposition. Contact annealing studies performed by Mergui et al. [182] indicate that some improvement in detector performance can be achieved through contact annealing. P–n and p–i–n junction detectors have also been formed through ion implantation [164,183], indium diffusion [164,184,185] and LPE growth [186,187], all with varying degrees of success.

Depletion layer studies on semi-insulating CdTe detectors indicate that non-uniform electric fields are present in some devices [188–190]. In some cases, the electric field did not extend completely across the device until appreciable voltage was applied. The non-uniform electric fields may be a consequence of single carrier injection or space charge polarization. Polarization can be a severe problem with CdTe devices if proper device processing techniques are not practiced [23,188,191,192]. Low resistivity detectors tend to suffer polarization effects less than high resistivity devices [160], and the problem can be reduced by using indium doped or low resistivity material. Illumination with infrared light [193] and various contact configurations [167,194] have reportedly helped to reduce polarization. Radiation-induced spectral changes have also been reported [191,195,196], in which the leakage current and temperature appear to have an effect on the degree of polarization [196]. Taguchi et al. [195] report observations of severely polarized detectors showing recovery after annealing at elevated temperatures (670 K).

CdTe detectors generally suffer from poor hole collection, hence resolution for large devices is degraded by position-dependent charge collection. Nevertheless, the literature is replete with examples of excellent RT gamma-ray energy resolution for small devices, generally 1–2 mm thick, with RT resolution as low as 1.7 keV FWHM for 59.5 keV gamma rays and 20 keV FWHM for 662 keV gamma rays (see for examples [5,23, 197,198]). Cooled devices demonstrate improved resolution [199], and recent results with compact thermoelectrically cooled CdTe detectors have shown gamma-ray energy resolution of 1.3 keV FWHM at 59.6 keV, 1.7 keV FWHM at 122 keV and 13 keV FWHM at 662 keV [200].

300 μm thick p–i–n detectors reported by Khusainov had energy resolution of 1.9 keV FWHM for 122 keV gamma rays, and 6.8 keV FWHM for 662 keV gamma rays, both at an operating temperature of −35°C [185]. Detectors with epitaxially formed HgCdTe contacts have also shown promising results [186,187], in which Ryan et al. [187] report RT energy resolution of 10.25 keV FWHM at 122 keV for 2 mm thick devices. The implanted junction detectors described by Cornet et al. [183] demonstrated RT energy resolution of 23 keV FWHM for ^{241}Am 5.5 MeV alpha particles.

CdTe detectors have been used as thermal neutron detectors in which prompt gamma ray emissions from the ^{113}Cd(n, γ)^{114}Cd reaction were observed [201–203]. The thermal neutron capture cross-section for ^{113}Cd, in which a multitude of gamma rays are released, is approximately 20 000 barns [201,202]. However, gamma rays of 558.6 and 651.3 keV are predominant, and the gamma-ray full energy peaks are clearly defined in a spectrum reported by Vradii et al. [203].

With suitable design and biasing of a hemisphere detector, the induced charge is primarily from electron transport and not holes [23,204,205]. Hage-Ali and Siffert [23,204] obtained RT energy resolution of 26 keV FWHM for 662 keV gamma rays taken with a 65 mm^3 active volume hemisphere detector. Pulse discrimination techniques have also been utilized to improve detector resolution for CdTe devices [23,204, 206–211]. As described by Jones and Woollam [206], short pulse lengths observed from the detector are correlated with electron transport, whereas long pulse lengths (in Ref. [206], greater than 100 ns) correspond to significant contributions to the induced charge from hole transport in which significant trapping effects can be apparent. By rejecting the long pulses and accepting only the shortened pulse lengths, the device can be operated as a single-carrier device. Unfortunately, pulse discrimination ultimately reduces the detector gamma-ray efficiency, as noted by Richter and Siffert [208], yet gamma-ray energy resolution can be dramatically improved. Pulse processing techniques with charge loss correction can help preserve detector efficiency, and RT resolution of 7.5 keV FWHM at 662 keV has been demonstrated for a 5 mm × 5 mm × 2 mm CdTe device (Fig. 8) [208]. A CdTe detector operated with pulse processing charge loss correction, described by Eisen and Horovitz [210], provided a RT energy resolution of 6.1 keV FWHM for 122 keV gamma rays, and as low as 6.4 keV FWHM for 356 keV gamma rays. Similar results were achieved with pulse shape selection and correction by Ivanov et al. [212].

CdTe detectors are commercially available and have been used for various applications in a number different fields. The list includes applications as medical instruments [213–220], heat shield ablation sensors [221], nuclear power station activity monitors [219,222], miniaturized nuclear fuel monitoring probes [223], capillary electrophoresis detectors [224], narcotics and explosive scanners [219], portable dosimeters [225,226], ammunition cartridge quality control monitors [220],
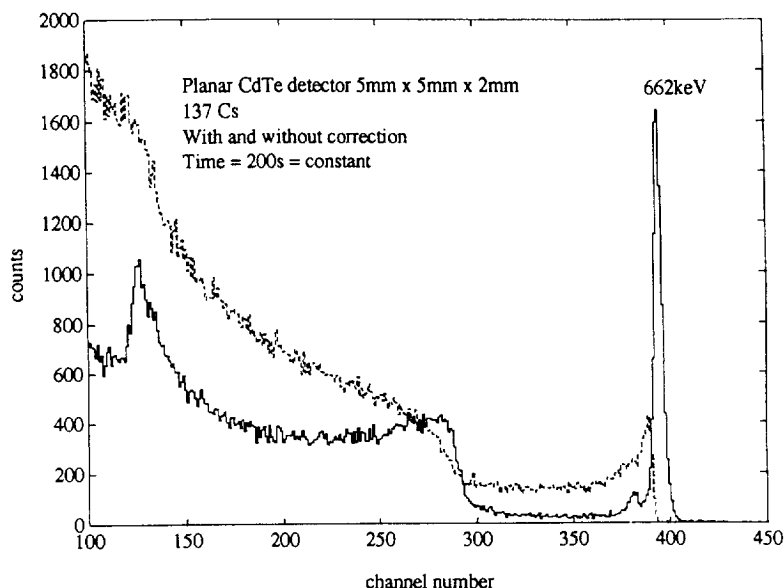

Fig. 8. ^{137}Cs spectrum measured with and without charge loss correction. The resolution is about 7.5 keV FWHM, the peak to Compton ratio is 3.4. For both spectra the measuring geometry and time have been the same (from Richter and Siffert [208]).

and a number of various configurations for X-ray and gamma-ray imaging [227–235].

6. Cd$_{1-x}$Zn$_x$Te detectors

The addition of Zn to the melt of Cd and Te during growth helps to reduce the dislocation density [236], thus producing higher quality substrate material for epitaxial growth. Hence, cadmium zinc telluride (Cd$_{1-x}$Zn$_x$Te) was introduced as an alternative substrate material for epitaxial HgCdTe growth [237]. Cd$_{1-x}$Zn$_x$Te has a cubic, zincblende lattice with atomic numbers of 48 (Cd), 30 (Zn) and 52 (Te), in which the photoelectric interaction probability is similar to CdTe. Relatively uniform, high resistivity (10^{10}–10^{11} Ω cm) Cd$_{1-x}$Zn$_x$Te material is generally produced through high-pressure Bridgman (HPB) growth with reported etch pit densities of 10^4/cm^2 [238,239]. The band gap energy dependency on the zinc concentration for Cd$_{1-x}$Zn$_x$Te at 300 K given by Olega et al. is [240,241]

$$E_0(x) = 1.510 + 0.606x + 0.139x^2 \text{ eV} \qquad (4)$$

in which the band gap energy of Cd$_{0.96}$Zn$_{0.04}$Te is near 1.534 eV, and the band gap energy for Cd$_{0.8}$Zn$_{0.2}$Te is near 1.637 eV. Elevated temperature tests on CdZnTe detectors yield an activation energy of 0.8 eV, indicating that the material is most likely compensated by a balance between deep and shallow levels [242]. The measured charge carrier mobilities for Cd$_{0.8}$Zn$_{0.2}$Te are 120 cm^2/V s for holes and 1350 cm^2/V s for electrons

[243]. The reported charge carrier mean free drift times range from 50 ns to 300 ns for holes, and range from 100 ns to 1 µs for electrons [165,243,256], thereby producing a condition in which position dependent charge collection can degrade energy resolution [9–12]. Optical measurements also indicate that the electric fields in CdZnTe devices with Schottky contact junctions are non-uniform [244], which can also effect detector performance.

The material described by Doty et al. [238] demonstrated higher sensitivity to gamma rays than CdTe crystals grown from purified Cd and Te, and similar CdZnTe material yields high gamma-ray energy resolution for relatively large crystals (by comparison with CdTe) [245–252]. The CdZnTe detectors are commonly fabricated by first polishing and etching slices with a dilute bromine/methanol mixture, and afterwards applying electrical contacts, usually with an electroless noble metal salt solution (such as AuCl$_3$, AgNO$_3$ or PtCl$_4$) [161,162,253]. There is some evidence that the choice of chemical etchant has an observable effect on detector spectroscopic performance. In the study, the best spectroscopic performance observed was from a detector etched with 5% bromine/methanol solution followed by a rinse in 2% bromine/20% lactic acid/ethylene glycol solution [254].

Fig. 9 shows a typical pulse height spectrum from a 5 mm × 5 mm × 2 mm Cd$_{0.8}$Zn$_{0.2}$Te detector, in which the RT energy resolution is 4.22 keV FWHM for 59.5 keV gamma rays. Devices (1.5 mm × 5 mm × 5 mm) with electroless AuCl$_3$ contacts provided RT energy resolutions of 2.89 keV FWHM for 60 keV gamma rays and 6.9 keV FWHM for 122 keV gamma rays [246]. Cd$_{0.8}$Zn$_{0.2}$Te detectors with dimensions of 3 mm × 3 mm × 2 mm have
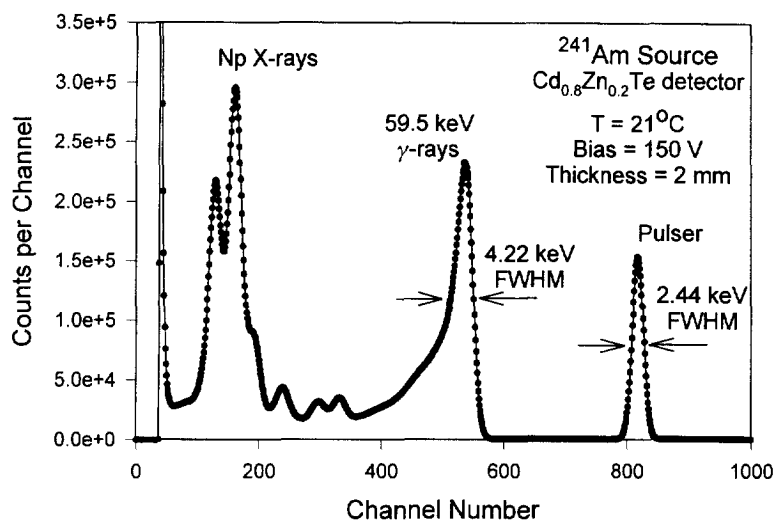
Fig. 9. Typical room-temperature (21°C) pulse height spectrum taken with a 5 mm × 5 mm × 2 mm Cd$_{0.8}$Zn$_{0.2}$Te gamma-ray detector. The applied bias is 150 V and the energy resolution is 4.22 keV FWHM for 59.5 keV gamma rays.
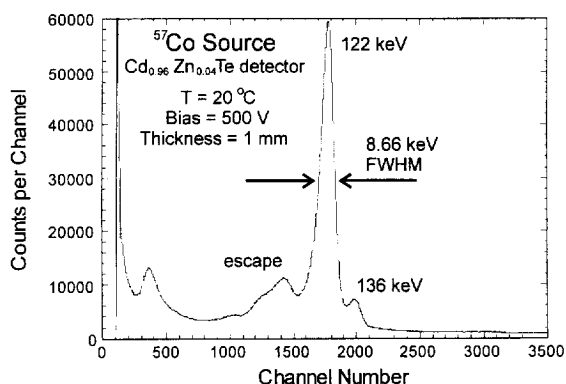
Fig. 10. Room-temperature (20°C) pulse height spectrum of [57]Co 122 keV and 136 keV gamma rays measured with a 1 mm thick Cd$_{0.96}$Zn$_{0.04}$Te p–SI–n detector. The reported resolution is 8.66 keV FWHM at 122 keV with a peak to valley ratio of 18.7 (from Hamilton et al. [251]).

given an energy resolution of 2.5 keV for 59.5 keV gamma rays [255]. High-resolution p–SI–n spectrometers fabricated from 1 mm thick, 10 mm^2 area Cd$_{0.96}$Zn$_{0.04}$Te samples with n- and p-type HgCdTe contacts gave RT energy resolution ranging from 3.35 to 8.66 keV FWHM for 122 keV gamma rays, and 6.46 keV FWHM for 356 keV gamma rays [250,251]. A representative [57]Co spectrum taken with a p–SI–n Cd$_{0.96}$Zn$_{0.04}$Te detector is shown in Fig. 10 (from Ref. [251]).

Thicker detectors generally suffer from incomplete hole collection, thus leading to gamma-ray pulse height spectra skewed towards lower energies. Several methods have been proposed to correct and reduce position-dependent charge collection effects, the most promising being pulse processing techniques [256–258] and single-charge-carrier-sensing devices [259–263]. Presently, pulse processing techniques used with a 18 mm × 18 mm × 2 mm Cd$_{0.9}$Zn$_{0.1}$Te device have reached a RT energy resolution of 9.3 keV FWHM for 662 keV gamma rays [256]. With an 18 mm × 18 mm × 5 mm Cd$_{0.9}$Zn$_{0.1}$Te detector, the RT energy resolution was 11.25 keV FWHM for 662 keV gamma rays [257]. Similar pulse processing techniques used for a 0.6 mm thick and 4 mm^2 Cd$_{0.9}$Zn$_{0.1}$Te detector at reduced temperature (−25°C) gave an energy resolution of 2.6 keV FWHM for 662 keV gamma rays [258]. Single charge-sensing devices utilize the concept demonstrated by Frisch [264], except that the sensing grid is applied on the semiconductor surface as a coplanar design. Single-charge-carrier-sensing devices have been successfully used with a 5 mm × 5 mm × 5 mm CdZnTe detector to demonstrate a RT energy resolution of less than 16.0 keV FWHM for 662 keV gamma rays [262,263]. Studies performed by He et al. [263,265] utilizing collimated ^{137}Cs gamma rays

indicate that energy resolution is best for interactions occurring near the cathode. Gamma-ray interactions occurring nearest the anode apparently degrade the overall energy resolution, yet recent results from He [265] show a RT energy resolution of 11.8 keV FWHM for 662 keV gamma rays as measured with a 1 cm^3 coplanar grid CdZnTe detector (Fig. 11).

A method which includes the coupling of multiple detectors in a stack has been shown to increase gamma-ray detection efficiency [266]. The charge collection efficiency for each device is slightly different, which gives a separate full energy peak in the pulse height spectrum from each detector for the same gamma ray energy. The problem is easily corrected with a shifting circuit, which allows the pulses from all of the detectors to be summed through a single preamplifier without the appearance of multiple peaks for any single energy [266]. Fig. 12 shows the pulse height spectrum from three stacked CdZnTe detectors before and after implementation of the shifting circuit.

Room-temperature Cd$_{0.8}$Zn$_{0.2}$Te detectors have recently been used successfully as thermal neutron detectors, in which unique gamma-ray emission lines from the [113]Cd(n, γ)[114]Cd were clearly identified [201,202,267]. The Cd$_{0.8}$Zn$_{0.2}$Te device demonstrated thermal neutron sensitivity of (3.7 ± 1.9)% for the 558.6 keV prompt gamma-ray emissions. Fig. 13 shows a [113]Cd(n, γ)[114]Cd emission spectrum taken with a Cd$_{0.8}$Zn$_{0.2}$Te detector placed in a thermal neutron beam from a reactor, displaying a RT energy resolution of 12.3 keV FWHM for 558.6 keV gamma rays. Recent studies indicate that CdZnTe is capable of withstanding fast neutron fluences up to 10^{10} n/cm^2 without suffering significant damage [268]; however gamma-ray spectra from activation products and resolution degradation become apparent at fluences above 10^{10} n/cm^2.

CdZnTe can operate reliably at elevated temperatures (up to 50°C [242]), with energy resolution for 81 keV gamma rays observed to increase from 8.91 keV FWHM at RT to 13.77 keV FWHM at 50°C. The apparent temperature stability allows for remote sensing, and remote sensor packs have been employed for real-time monitoring of special nuclear materials (SNM) [269–271]. The devices operate mainly as counters, in which lower grade and relatively inexpensive CdZnTe material performs well. Under special occasions, high-resolution CdZnTe spectrometers can be utilized for SNM identification [250,270,272]. CdZnTe detectors with RT energy resolution of 4.04 keV FWHM for 186 keV [235]U gamma rays have been reported [250]. By measuring the ratio of [235]U and [238]U emissions, RT CdZnTe spectrometers can be used to determine the enrichment, presently with a reported accuracy near 10% [272]. CdZnTe detectors have also become very attractive for X-rays and gamma-ray imaging systems, and for medical applications [273–281].
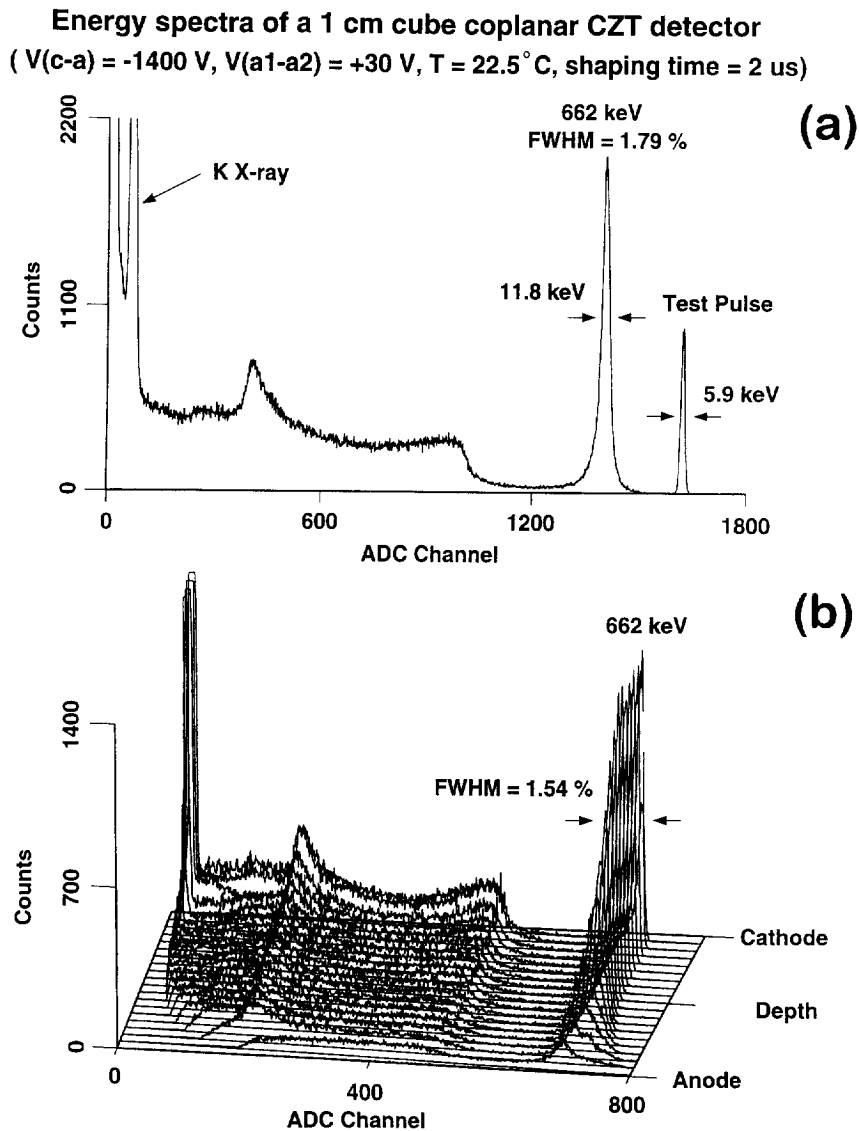
Energy spectra of a 1 cm cube coplanar CZT detector
(V(c-a) = -1400 V, V(a1-a2) = +30 V, T = 22.5°C, shaping time = 2 us)

Fig. 11. Room-temperature pulse height spectrum of ^{137}Cs 662 keV gamma rays measured with a 1 cm^3 CdZnTe coplanar grid detector. As shown, energy resolution is best for gamma ray interactions near the cathode. The overall RT energy resolution is 11.8 keV FWHM at 662 keV (from He [265]).

7. Other compound semiconductor detectors

The properties of lead iodide (PbI$_2$) indicate that it is a promising ambient temperature radiation detector [282–291]. The material forms in the hexagonal, close-packed (HCP) lattice with a mass density of 6.2 g/cm^3 [292–294]. The band gap energy is 2.55 eV, and the reported charge carrier mobilities are 8 cm^2/V s for electrons and 2 cm^2/V s for holes [284]. The relatively large band gap energy indicates that devices should operate with low leakage currents at elevated temperatures. Early results from PbI$_2$ detectors indicated that charge carrier mean free drift times were short, and the devices demonstrated satellite energy peaks for alpha particles [284]. Zone refinement purification of PbI$_2$ starting material has reportedly improved radiation spectrometer performance [285–287]. Detectors have been fabricated by various methods and samples are generally cleaved with a fine blade [285–287], or sliced with a string saw [291]. Detector contacts have been fabricated from Au, Pd and
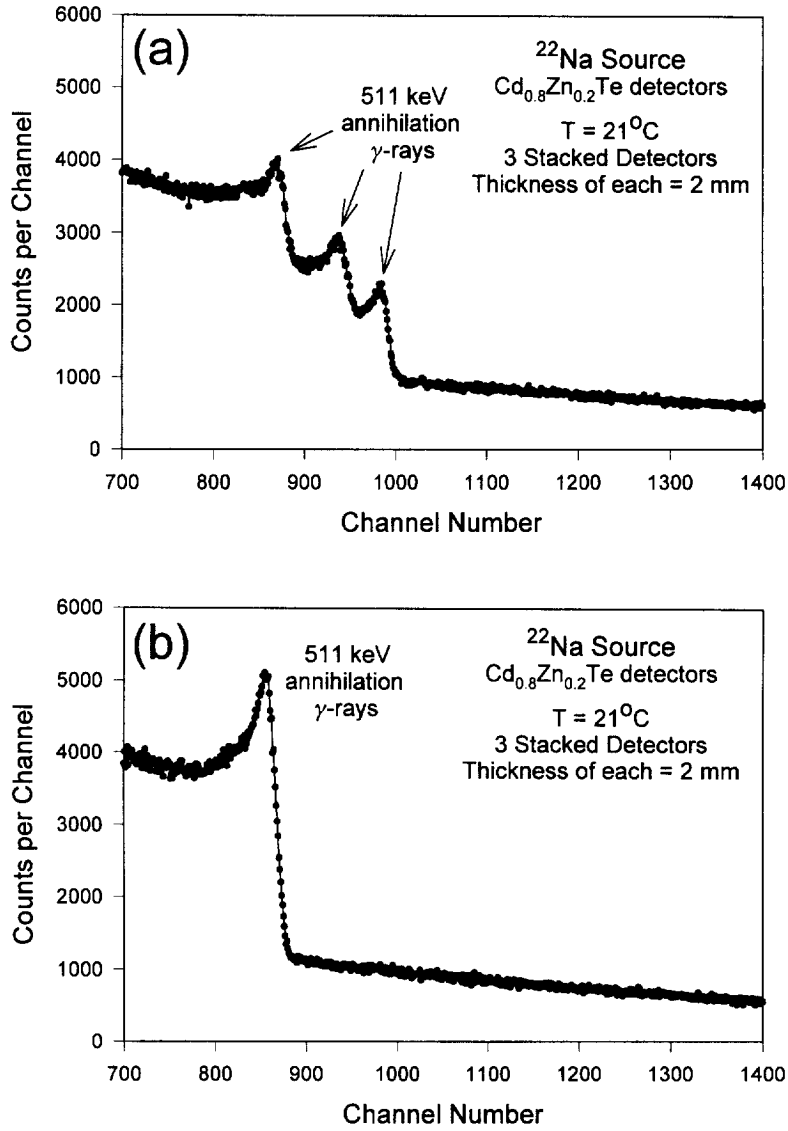
Fig. 12. Room-temperature (21°C) spectra of ^{22}Na 511 keV annihilation gamma rays taken with a stack of three 5 mm × 5 mm × 2 mm $Cd_{0.8}Zn_{0.2}Te$ gamma-ray detectors, in which (a) three separate peaks appear as a result of differences in charge collection efficiency from the three detectors, and (b) the peaks are shifted to the same location with the circuit described by Olsen et al. [266].

Aquadag (colloidal carbon) with similar results [287,291]. Recent results give charge carrier mean free drift times ∼1 µs for electrons and 0.3 µs for holes [291]. Reported RT energy resolution for a 107 µm thick device was 712 eV FWHM for 5.9 keV gamma rays and 1.83 keV FWHM for 59.5 keV gamma rays (see Fig. 14) [291].

Indium phosphide (InP) has received some attention as a possible radiation detector [295–298]. InP has atomic numbers of 49/15 with a mass density of 4.79 g/cm^3. With a band gap energy of only 1.35 eV, relatively high thermal generation currents can render the material unsuitable for large devices. The theoretical charge carrier mobilities for high-quality InP are 4600 cm^2/V s for electrons and 150 cm^2/V s for holes [18]. The average ionization energy of InP is 4.2 eV/e–h pair [299,300]. It has been speculated that the relatively large neutrino cross-section of ^{115}In (in a reaction leading to beta particle and low-energy gamma-ray emissions [301]), can be exploited in InP neutrino detectors [295–297].
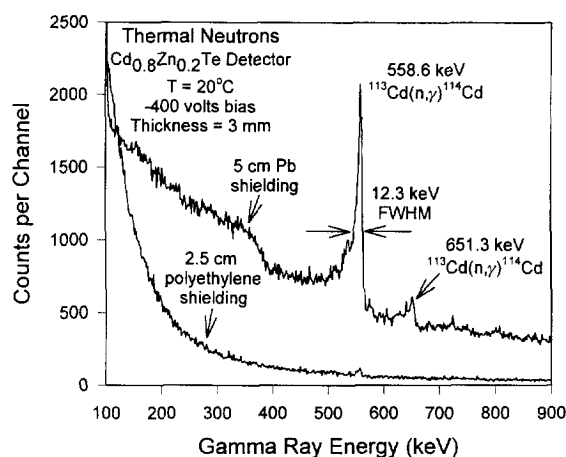
Fig. 13. Room-temperature pulse height spectrum measured with a 10 mm × 10 mm × 3 mm $Cd_{0.8}Zn_{0.2}Te$ detector placed in a reactor thermal neutron beam, in which the neutrons were detected through the $^{113}Cd(n, \gamma)^{114}Cd$ reaction. Different attenuators were placed in the thermal neutron beam before the detector. With 2.5 cm of high density polyethylene in the beam, the neutrons are scattered before reaching the detector, hence no spectrum is observed. Neutrons pass through 10 cm of Pb, yet background gamma rays are attenuated; hence the 558.6 and 651.3 keV prompt gamma-ray emissions are definitely from neutron interactions in the detector.

Unfortunately, the substantially large volume of InP necessary for a viable neutrino detector (well over 1 m³) is presently not practical. Additionally, background radiation would be difficult to discriminate from neutrino events for such a device. InP detectors have been shown to be sensitive to beta particles [295], alpha particles [297,298], and low-energy gamma rays [297]. Charge carrier trapping presently limits their use as an alternative radiation spectrometer. InP detectors have found most use as high-speed radiation pulse detectors [302–309], in which the short carrier mean free drift times are beneficial. A time resolution of less than 200 ps (FWHM) has been achieved with, for example, InP(Fe) detectors in this application [306–309].

Cadmium selenide (CdSe), another possible RT low-energy gamma ray and X-ray detector [310–314], has atomic numbers of 48/34 with a mass density of 5.8 g/cm³. Canali et al. [315] have measured the electron and hole mobilities for CdSe as 720 and 75 cm²/V s, respectively. The band gap energy of CdSe is 1.73 eV and the crystal structure is Wurtzite [314]. Small CdSe detectors (0.2 and 1 mm thick) have demonstrated a RT energy resolution of 1.4 keV FWHM for 5.9 keV gamma rays, and 8.5 keV FWHM for 59.5 keV gamma rays [314]. The substantial hole trapping observed in present day material limits the detector usage to low-energy
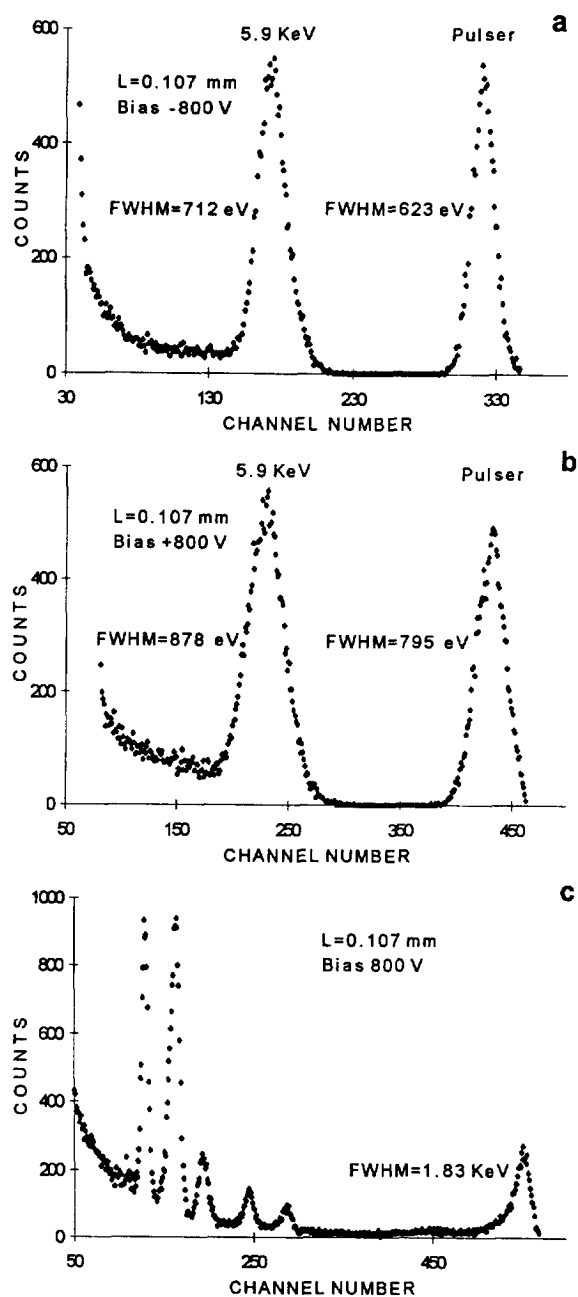

Fig. 14. Spectra of the ^{55}Fe isotope (5.9 keV), with negative (a) and positive (b) bias applied to the irradiated side of the crystal, and (c) of the ^{241}Am isotope (59.6 keV – highest energy peak) obtained with a lead iodide detector (from Deich and Roth [291]).

gamma-ray spectroscopy. Ternary $Cd_{0.7}Zn_{0.3}Se$ compounds have also been investigated for radiation detectors [316,317]. The addition of Zn increases the band gap energy, thereby decreasing leakage currents. Small

devices performed similarly to CdSe detectors, with reported RT energy resolution of 1.8 keV FWHM for 5.9 keV gamma rays, and 4.0 keV FWHM for 27.4 keV gamma rays [317]. Carrier transport and trapping presently limits the use of CdSe and $Cd_{0.7}Zn_{0.3}Se$ as a detector material, and CdSe and $Cd_{0.7}Zn_{0.3}Se$ detectors are not commercially available.

Gallium selenide (GaSe) was studied as a possible RT radiation detector in the mid-1970s [318–320]. The material has atomic numbers of 31/34 with a density of 4.55 g/cm³. The crystal has a layered structure with a sequence of covalently bonded Se–Ga–Ga–Se layers held together by van der Waals bonds, and the band gap energy is 2.03 eV. Manfredotti et al. [318] report electron and hole mobilities of 60 and 215 cm²/V s, respectively, and an energy resolution for a GaSe particle detector of 370 keV FWHM for 5.486 MeV alpha particles. These results may be compared with those of Sakai et al. [321] who obtained charge carrier mobilities of 70 cm²/V s for electrons and 45 cm²/V s for holes, and a best RT energy resolution of 250 keV FWHM for 5.486 MeV alpha particles. Yamazaki et al. [323] report RT energy resolution for GaSe detectors ranging between 220 and 820 keV FWHM for 5.486 MeV alpha particles. Sakai et al. [321] and Nakatani et al. [322] also report the average ionization energy for GaSe to be between 4.0 and 4.5 eV/e–h pair. GaSe has also been explored as a high dose sensitivity X-ray detector [324]. Resolution degradation and the appearance of satellite peaks with GaSe detectors [318], probably due to material inhomogeneities and charge carrier trapping, mean that substantial improvement is required before its use as a viable alternative radiation detector. At present, GaSe devices are experimental and are not commercially available.

Thallium halide compound semiconductors have been investigated as possible RT gamma-ray detectors [325–330]. TlBr has atomic numbers of 81/35 and a mass density of 7.5 g/cm³. The band gap energy of TlBr is 2.68 eV, implying that detectors should operate at elevated temperatures with low leakage currents, and the high atomic number of Tl yields a relatively high photoelectric absorption cross-section. Early devices reported by Rahman et al. [325,326] had poor energy resolution for charged particles and only operated at reduced temperatures. An energy resolution of 1.5 keV FWHM for 5.9 keV gamma rays (temperature not reported) has been achieved with small devices [329]. The ternary halide $TlBr_{0.35}I_{0.65}$ has also been investigated as a photodetector for various scintillators, including CsI(Tl) [330]. The RT alpha particle energy resolution for the CsI(Tl)/$TlBr_{0.35}I_{0.65}$ device was poor, however, at ∼1.12 MeV FWHM for 5.486 MeV alpha particles.

Cubic boron phosphide (BP), with a band gap energy of 2.1 eV, has unique properties that seem ideal for solid-state RT thermal neutron detectors [331–334]. ^{10}B (21% natural abundance) has a high thermal neutron cross-section (3840 barns), and the $^{10}B(n, \alpha)^7Li$ reaction releases energetic alpha particles and Li ions that can be easily detected [7]. Additionally, since the material is composed of low atomic number elements (5/15), background gamma-ray interactions can be minimized. Although the required growth parameters for BP can present several difficulties with bulk crystal growth [335–338], a ^{10}BP film only 200 µm thick will absorb over 95% of incident thermal neutrons, and CVD-grown BP films of such a thickness have already been realized [339,340]. At present, CVD-grown BP films have high impurity levels which render the material n-type or p-type and diodes fabricated from the CVD-grown films break down with only a few volts of applied bias [341,342]. The material shows promise, but further material improvements are required before practical neutron detectors can be realized.

Other compound semiconductors that have been studied include AlSb [343–346], CdS [347], ZnSe [348,349], InI [350,351], GaP [352] and SiC [353]. Most of these alternative compound semiconductor materials being studied as radiation detectors suffer severely from high concentrations of impurities and traps, and they are generally not commercially available. Various reports have recommended select compound semiconductors as having the best combination of properties for RT radiation spectrometers [14,15,354]. AlSb has been suggested as an ideal RT gamma ray spectrometer material [14,15,343], yet the material has proven to be difficult to grow and it tends to decompose when exposed to air and water moisture [345]. CdSe has also been cited as an ideal RT operated detector [354]; however, practical CdSe detectors have not yet been realized due to difficulties with producing high-quality CdSe material.

8. Concluding remarks

CdTe, HgI_2 and CdZnTe radiation detectors are commercially available and have demonstrated good room temperature gamma-ray and charged particle energy resolution. The individual devices are mostly restricted to small sizes, however, and large detecting systems are composed of multiple element arrays. High-quality devices also tend to be relatively expensive, tending to reduce compound semiconductor detector utilization to specialized applications in which Ge, Si, or scintillation detectors are unsuitable.

Although some novel detector designs increase detector energy resolution, ultimately the quality of the materials themselves must be improved in order to produce the substantial detector volume increases that are required for efficient, high-resolution radiation spectrometers. Observing that the concept of using compound semiconductors as radiation detectors was introduced in 1945, it becomes clear that material improvements are

much easier to discuss than to implement. Some compound semiconductors mentioned in the present review (such as BP for neutron detectors), have tremendous promise, yet material growth and production issues render the development slow and cost recovery risky. Previous review authors have alluded to the fact that progress in the field of compound semiconductor detectors is slow due to the lack of funding and, for that matter, lack of widespread interest in the development for other applications [16,17]. Nevertheless, energy resolution and detector performance have consistently improved over the years, and compound semiconductor radiation detectors are presently being utilized for a growing number of different applications. It can only be expected that several of the detector materials discussed will continue to find increasing use in the future.

Acknowledgements

References

[1] P.J. Van Heerden, The Crystal Counter, Utrecht Dissertation, 1945.
[2] R. Hofstadter, Nucleonics 4 (1949) 2.
[3] R. Hofstadter, Nucleonics 4 (1949) 29.
[4] A.G. Chynoweth, Am. J. Phys. 20 (1952) 218.
[5] W.J. Price, Nuclear Radiation Detection, McGraw-Hill, New York, 1958.
[6] W.J. Price, Nuclear Radiation Detection, 2nd ed., McGraw-Hill, New York, 1964.
[7] G.F. Knoll, Radiation Detection and Measurement, 2nd ed., Wiley, New York, 1989.
[8] J.W. Mayer, Nucl. Instr. and Meth. 43 (1966) 55.
[9] R.B. Day, G. Dearnaley, J.M. Palms, IEEE Trans. Nucl. Sci. NS-14 (1967) 487.
[10] N.B. Strokan, V.K. Yeryomin, S.A. Lomashevich, N.I. Tisnek, IEEE Trans. Nucl. Sci. NS-19 (3) (1972) 365.
[11] W. Akutagawa, K. Zanio, J. Appl. Phys. 40 (1969) 3838.
[12] G.F. Knoll, D.S. McGregor, MRS Proc. 302 (1993) 3.
[13] R.B. Hammond, N.G. Paulter, A.E. Iverson, R.C. Smith, Tech. Dig. Int. Electron Devices Meeting (1981) 157.
[14] S.P. Swierkowski, G.A. Armantrout, IEEE Trans. Nucl. Sci. NS-22 (1975) 205.

[15] G.A. Armantrout, S.P. Swierkowski, J.W. Sherohman, J.H. Yee, IEEE Trans. Nucl. Sci. NS-24 (1977) 121.
[16] E. Sakai, Nucl. Instr. and Meth. 196 (1982) 121.
[17] M. Cuzin, Nucl. Instr. and Meth. A 253 (1987) 407.
[18] S.M. Sze, Physics of Semiconductor Devices, 2nd ed., Wiley, New York, 1981.
[19] W. Shockley, J. Appl. Phys. 9 (1938) 635.
[20] S. Ramo, Proc. IRE 27 (1939) 584.
[21] K. Hecht, Z. Physik 77 (1932) 235.
[22] E. Sakai, IEEE Trans. Nucl. Sci. NS-15 (1968) 310.
[23] M. Hage-Ali, P. Siffert, CdTe Nuclear Detectors and Applications, in: T.E. Schlesinger, R.B. James (Eds.), Semiconductors for Room Temperature Nuclear Detector Applications, Semiconductors and Semimetals, vol. 43, Academic Press, San Diego, 1995.
[24] V. Radeka,. IEEE Trans. Nucl. Sci. NS-21 (1974) 51.
[25] V. Radeka, Ann. Rev. Nucl. Part. Sci. 38 (1988) 217.
[26] F.J. Walter, Proc. Asheville Conf., NAS-NRC, Publ. 871, 1961, p. 237.
[27] W.R. Dodge, S.R. Domen, A.T. Hirshfeld, D.D. Hoppes, IEEE Trans. Nucl. Sci. NS-12 (1965) 295.
[28] R. Stuck, J.P. Ponpon, P. Siffert, C. Ricaud, IEEE Trans. Nucl. Sci. NS-19 (1972) 270.
[29] S. Kavaldias, K. Misiakos, D. Loukas, E. Tsoi, Nucl. Instr. Meth. A 322 (1992) 562.
[30] U. Fano, Phys. Rev. 72 (1947) 26.
[31] W.R. Harding, C. Hilsum, M.E. Moncaster, D.C. Northrop, O. Simpson, Nature 187 (1960) 405.
[32] A. Barraud, Comptes Rendus 257 (1963) 1263.
[33] J.E. Eberhardt, R.D. Ryan, A.J. Tavendale, Appl. Phys. Lett. 17 (1970) 427.
[34] J.E. Eberhardt, R.D. Ryan, A.J. Tavendale, Proc. Int. Symp. Cadmium Telluride, Strasbourg, Paper no. 29, 1971.
[35] J.E. Eberhardt, R.D. Ryan, A.J. Tavendale, Nucl. Instr. and Meth. 94 (1971) 463.
[36] T. Kobayashi, T. Sugita, M. Koyama, S. Takayanagi, IEEE Trans. Nucl. Sci. NS-19 (1972) 324.
[37] K. Hesse, W. Gramann, Proc. Int. Symp. Cadmium Telluride, Strasbourg, Paper no. 30, 1971.
[38] P.E. Gibbons, J.H. Howes, IEEE Trans. Nucl. Sci. NS-19 (1972) 353.
[39] K. Hesse, W. Gramann, D. Höppner, Nucl. Instr. and Meth. 101 (1972) 39.
[40] T. Kobayashi, T. Sugita, S. Takayanagi, M. Iio, Y. Sasaki, IEEE Trans. Nucl. Sci. NS-20 (1973) 310.
[41] T. Kobayashi, I. Kuru, A. Hojo, T. Sugita, NS-23 (1976) 97.
[42] D.S. McGregor, J.E. Kammeraad, in: Semiconductors for Room Temperature Nuclear Detector Applications, T.E. Schlesinger, R.B. James (Eds.), Semiconductors and Semimetals, vol. 43, Academic Press, San Diego, 1995.
[43] D. Alexiev, K.S.A. Butcher, Nucl. Instr. and Meth. A 317 (1992) 111.
[44] T.J. Sumner, S.M. Grant, D. Alexiev, K.S.A. Butcher, Nucl. Instr. and Meth. A 348 (1994) 518.
[45] J. Lauter, D. Protic, A. Förster, H. Lüth, Nucl. Instr. and Meth. A 356 (1995) 324.
[46] G.M. Martin, A. Mitonneau, A. Mircea, Electron. Lett. 77 (1977) 191.

[47] D.E. Holmes, R.T. Chen, K.R. Elliott, C.G. Kirkpatrick, Appl. Phys. Lett. 40 (1982) 46.

[48] R.K. Willardson, A.C. Beer (Eds.), in: Semiconductors and Semimetals, vol. 20, Academic Press, Orlando, 1984.

[49] D.S. McGregor et al., IEEE Trans. Nucl. Sci., NS-43 (1996) 1397.

[50] D.S. McGregor, G.F. Knoll, Y. Eisen, R. Brake, IEEE Trans. Nucl. Sci. NS-39 (1992) 1226.

[51] K. Berwick, M.R. Brozel, C.M. Buttar, M. Cowper-thwaite, Y. Hou, MRS Proc. 302 (1993) 363.

[52] K. Berwick, M.R. Brozel, C.M. Buttar, M. Cowper-thwaite, Y. Hou, Inst. Phys. Conf. Series 135 (1993) 305.

[53] D.S. McGregor, R.A. Rojeski, G.F. Knoll, F.L. Terry, Jr., J. East, Y. Eisen, Nucl. Instr. and Meth. A 343 (1994) 527.

[54] S.B. Beaumont et al., Nucl. Phys. B, Proc. Suppl. 32 (1993) 296.

[55] M. Alietti et al., Nucl. Instr. and Meth. A 355 (1995) 420.

[56] V. Ya. Prinz, B.A. Bobylev, Sov. Phys. Semicond. 14 (1980) 1097.

[57] V. Ya. Prinz, S.N. Rechkunov, Phys. Stat. Sol. (b) 118 (1983) 159.

[58] F. Piazza, P.C.M. Christianen, J.C. Maan, Appl. Phys. Lett. 69 (1996) 1909.

[59] D.S. McGregor, R.A. Rojeski, G.F. Knoll, F.L. Terry, Jr., J. East, Y. Eisen, J. Appl. Phys. 75 (1994) 7910; errata: D.S. McGregor, R.A. Rojeski, G.F. Knoll, F.L. Terry, Jr., J. East, Y. Eisen, J. Appl. Phys. 77 (1994) 1331.

[60] I.L. Donnelly, M.L. Williams, these Proceedings (4th Int. Workshop on GaAs Detectors and Related Compounds, Aberfoyle, Scotland, 1996) Nucl. Instr. and Meth. A 395 (1997) 9.

[61] A. Cola, L. Vasanelli, L. Reggiani, A. Cavallini, F. Nava, Ref. [60], p. 98.

[62] T. Kubicki, K. Lübelsmeyer, J. Ortmanns, D. Pandoulas, O. Syben, M. Toporowsky, W.J. Xiao, Nucl. Instr. and Meth. A 345 (1994) 468.

[63] J.W. Chen et al., Nucl. Instr. and Meth. A 365 (1995) 273.

[64] M. Alietti et al., Nucl. Instr. and Meth. A 362 (1995) 344.

[65] S. King et al., IEEE Trans. Nucl. Sci. NS-43 (1996) 1376.

[66] A.D. Holland, A.D.T. Short, T. Cross, Nucl. Instr. and Meth. A 346 (1994) 366.

[67] G. Bertuccio, M. Alietti, C. Canali, A. Cetronio, C. Chiossi, F. Nava, Nucl. Instr. and Meth. A 379 (1996) 152.

[68] K. Berwick, M.R. Brozel, C.M. Buttar, J.S. Pooni, P.J. Sellin, S.M. Young, Nucl. Instr. and Meth. A 380 (1996), 46.

[69] C. del Papa, P.G. Pelfer, K. Smith (Eds.), GaAs Detectors and Electronics for High Energy Physics, World Scientific, Singapore, 1992.

[70] S.P. Beaumont et al., Nucl. Instr. and Meth. A 322 (1992) 472.

[71] S.P. Beaumont et al., IEEE Trans. Nucl. Sci. NS-40 (1993) 1225.

[72] S.P. Beaumont et al., Nucl. Instr. and Meth. A 348 (1994) 514.

[73] W. Braunschweig et al., Nucl. Instr. and Meth. A 370 (1996) 377.

[74] R. Bates et al., IEEE Trans. Nucl. Sci. NS-43 (1996) 1137.

[75] A.L. Barry, R. Wojcik, A.L. MacDiarmid, IEEE Trans. Nucl. Sci. NS-36 (1989) 2400.

[76] E. Bertolucci et al., Nucl. Instr. and Meth. A 362 (1995) 547.

[77] D.S. McGregor, J.T. Lindsay, C.C. Brannon, R.W. Olsen, IEEE Trans. Nucl. Sci. NS-43 (1996) 1357.

[78] D.R. Kania, S.M. Lane, S.G. Prussin, Appl. Phys. Lett. 53 (1988) 1988.

[79] C.L. Wang, M.D. Pocha, J.D. Morse, M.S. Singh, B.A. Davis, Appl. Phys. Lett. 54 (1989) 1451.

[80] C.L. Wang, J.E. Flatley, M.D. Pocha, Energy Tech. Rev. (1991) 15.

[81] A. Friant, C. Saliou, R. Galli, S. Barday, Nucl. Instr. and Meth. A 283 (1989) 318.

[82] B. Brullot, R. Galli, X. Lecat, C. Rubbelynck, T. Pochet, MRS Proc. 302 (1993) 369.

[83] F. Foulon, B. Brullot, C. Rubbelynck, P. Bergonzo, T. Pochet, IEEE Trans. Nucl. Sci. NS-43 (1996) 1372.

[84] J. Lauter, A. Förster, L. Lüth, K.D. Müller, R. Reinartz, IEEE Trans. Nucl. Sci. NS-43 (1996) 1446.

[85] W.R. Willig, Nucl. Instr. and Meth. 96 (1971) 615.

[86] W.R. Willig, Nucl. Instr. and Meth. 101 (1972) 23.

[87] H.L. Malm, IEEE Trans. Nucl. Sci. NS-19(3) (1972) 263.

[88] S.P. Swierkowsky, G.A. Armantrout, R. Wichner, Appl. Phys. Lett. 23 (1973) 281.

[89] S.P. Swierkowsky, G.A. Armantrout, R. Wichner, IEEE Trans. Nucl. Sci. NS-21(1) (1974) 302.

[90] J.L. Llacer, M.K. Watt, M. Schieber, R. Carlsten, D. Schnepple, IEEE Trans. Nucl. Sci. NS-21(1) (1974) 305.

[91] J.P. Ponpon, R. Stuck, P. Siffert, C. Schwab, Nucl. Instr. and Meth. 119 (1974) 197.

[92] J.P. Ponpon, R. Stuck, P. Siffert, B. Meyer, C. Schwab, IEEE Trans. Nucl. Sci. NS-22 (1975) 182.

[93] G.R. Ricker, J.V. Vallerga, A.J. Dabrowski, J.S. Iwanczyk, G. Entine, Rev. Sci. Instr. 53 (1982) 700.

[94] A. Burger, D. Nason, L. van den Berg, M. Scheiber, in: Seimconductors for Room Temperature Nuclear Detector Applications, T.E. Schlesinger, R.B. James (Eds.), Semiconductors and Semimetals, vol. 43 Academic Press, San Diego, 1995.

[95] H. Hermon, M. Roth, M. Schieber, J. Shamir, Mat. Res. Bull. 28 (1993) 229.

[96] I.F. Nicolau, J.P. Joly, J. Crystal Growth 48 (1980) 61.

[97] A. Friant, J. Mellet, C. Saliou, T. Mohammad Brahim, IEEE Trans. Nucl. Sci. NS-27 (1980) 281.

[98] J. Mellet, A. Friant, Nucl. Instr. and Meth. A 283 (1989) 199.

[99] H. Scholz, Acta Electronica, 17 (1974) 69.

[100] M. Schieber, W.F. Schnepple, L. Van Den Berg, J. Crystal Growth 33 (1976) 125.

[101] M. Schieber, I. Beinglass, G. Dishon, A. Holzer, G. Yaron, Nucl. Instr. and Meth. 150 (1978) 71.

[102] H. Hermon, M. Roth, M. Schieber, Nucl. Instr. and Meth. A 322 (1992) 432.

[103] W. Li et al., IEEE Trans. Nucl. Sci. NS-43 (1996) 1369.

[104] Y.F. Nicolau, Nucl. Instr. and Meth. 213 (1983) 13.

[105] S.P. Faile, A.J. Dabrowski, G.C. Huth, J.S. Iwanczyk, J. Crystal Growth 50 (1980) 752.

[106] B. Coupat, J.P. Fournier, M. Silga, J. Omaly, Nucl. Instr. and Meth. A 269 (1988) 213.

[107] J. Przyluski, J. Laskowski, Nucl. Instr. and Meth. A 283 (1989) 144.

[108] L. Van Den Berg, W.F. Schnepple, Nucl. Instr. and Meth. A 283 (1989) 335.

[109] R. Cadoret, P. Brisson, A. Magnan, Nucl. Instr. and Meth. A 283 (1989) 339.

[110] L. Van Den Berg, MRS Proc. 302 (1993) 73.

[111] M. Schieber, Nucl. Instr. and Meth. 144 (1977) 469.

[112] V.M. Gerrish, in: T.E. Schlesinger, R.B. James (Eds.), Semiconductors for Room Temperature Nuclear Detector Applications, Semiconductors and Semimetals, vol. 43, Academic Press, San Diego, 1995.

[113] R. Scott, Appl. Phys. Lett. 27 (1975) 99.

[114] M. Slapa, G.C. Huth, W. Seibt, M.M. Scheiber, P.T. Randtke, IEEE Trans. Nucl. Sci. NS-23 (1976) 102.

[115] A. Holzer, M. Scheiber, IEEE Trans. Nucl. Sci. NS-27 (1980) 266.

[116] T. Mohammid-Brahim, A. Friant, J. Mellet, IEEE Trans. Nucl. Sci. NS-32 (1984) 581.

[117] V. Gerrish, Nucl. Instr. and Meth. A 322 (1992) 402.

[118] T.E. Schlesinger, X.J. Bao, R.B. James, A.Y. Cheng, C. Ortale, L. van den Berg, Nucl. Instr. and Meth. A 322 (1992) 414.

[119] J.S. Iwanczyk, W.F. Schnepple, M.J. Masterson, Nucl. Instr. and Meth. A 322 (1992) 421.

[120] V. Gerrish, Proc. MRS 302 (1993) 129.

[121] X.J. Bao, R.B. James, T.E. Schlesinger, in: T.E. Schlesinger, R.B. James (Eds.), Semiconductors for Room Temperature Nuclear Detector Applications, Semiconductors and Semimetals, vol. 43, Academic Press, San Diego, 1995.

[122] X.J. Bao, R.B. James, T.E. Schlesinger, in: T.E. Schlesinger, R.B. James (Eds.), Semiconductors for Room Temperature Nuclear Detector Applications, Semiconductors and Semimetals, vol. 43, Academic Press, San Diego, 1995.

[123] B.E. Patt, J.S. Iwanczyk, G. Vilkelis, Y. Wang, Nucl. Instr. and Meth. A 380 (1996) 276.

[124] F.D. Becchetti, R.S. Raymond, R.A. Ristinen, W.F. Schnepple, C. Ortale, Nucl. Instr. and Meth. 213 (1983) 127.

[125] J.S. Iwanczyk, J.B. Barton, A.J. Dabrowski, J.H. Kusmiss, W.M. Szymczyk, IEEE Trans. Nucl. Sci. N-30 (1983) 363.

[126] J.S. Iwanczyk, J.B. Barton, A.J. Dabrowski, J.H. Kusmiss, W.M. Szymczyk, G.C. Huth, J. Markakis, W.F. Schnepple, R. Lynn, Nucl. Instr. and Meth. 213 (1983) 123.

[127] J. Bornstein, R.H. Bube, J. Appl. Phys. 61 (1987) 2676.

[128] J. Markakis, C. Ortale, W. Schnepple, J. Iwanczyk, A. Dabrowski, IEEE Trans. Nucl. Sci. NS-32 (1985) 559.

[129] J.M. Markakis, IEEE Trans. Nucl. Sci. NS-35 (1988) 356.

[130] J.M. Markakis, Nucl. Instr. and Meth. A 263 (1988) 499.

[131] J.M. Markakis, A.Y. Cheng, Nucl. Instr. and Meth. A 283 (1989) 236.

[132] Y.J. Wang, J.S. Iwanczyk, B.E. Patt, IEEE Trans. Nucl. Sci. NS-41 (1994) 910.

[133] Y.J. Wang, B.E. Patt, J.S. Iwanczyk, Nucl. Instr. and Meth. A 353 (1994) 50.

[134] Y.J. Wang, B.E. Patt, J.S. Iwanczyk, S.R. Cherry, Y. Shao, IEEE Trans. Nucl. Sci. NS-42 (1995) 601.

[135] Y.J. Wang, B.E. Patt, J.S. Iwanczyk, S.R. Cherry, Y. Shao, IEEE Trans. Nucl. Sci. NS-43 (1996) 1277.

[136] C. Ortale, L. Padget, W.F. Schepple, Nucl. Instr. and Meth. 213 (1983) 95.

[137] B.E. Patt, A. Del Duca, R. Dolin, C. Ortale, IEEE Trans. Nucl. Sci. NS-33 (1986) 523.

[138] J.S. Iwanczyk, W.K. Warburton, B. Hedman, K.O. Hodgson, A. Beyerle, Nucl. Instr. and Meth. A 266 (1988) 619.

[139] J.S. Iwanczyk, W.K. Warburton, A.J. Dabrowski, B. Hedman, K.O. Hodgson, B.E. Patt, IEEE Trans. Nucl. Sci. NS-35 (1988) 93.

[140] B.E. Patt, A.G. Beyerle, R.C. Dolin, C. Ortale, Nucl. Instr. and Meth. A 283 (1989) 215.

[141] W. Dusi, E. Caroli, G. Di Cocco, A. Donati, G. Landini, G. Ramunno, M. Amann, J.M. Koebel, P. Siffert, D. Grassi, E. Perillo, Nucl. Instr. and Meth. A 348 (1994) 531.

[142] B.E. Patt, J.S. Iwanczyk, R. Szczebiot, G. Maculewicz, M. Wang, Y.J. Wang, B. Hedman, K.O. Hodgson, A.D. Cox, IEEE Trans. Nucl. Sci. NS-42 (1995) 558.

[143] J.S. Iwanczyk, B.E. Patt, Y.J. Wang, M. Croft, Z. Kalman, W. Mayo, IEEE Trans. Nucl. Sci. NS-42 (1995) 606.

[144] W. Dusi, E. Caroli, A. Donati, C. Olivieri, G. Ramunno, D. Grassi, E. Perillo, G. Spadaccini, M. Amann, J.M. Koebel, P. Siffert, Nucl. Instr. and Meth. A 369 (1996) 141.

[145] S. Caine, A. Holzer, I. Beinglass, M. Schieber, E. Lowenthal, IEEE Trans. Nucl. Sci. NS-25 (1978) 649.

[146] A. Levi, M. Roth, M. Schieber, S. Lavy, G. Cooper, IEEE Trans. Nucl. Sci. NS-29 (1982) 457.

[147] Dahlbom, M.A. Mandelkern, E.J. Hoffman, A.R. Ricci, J.B. Barton, J.S. Iwanczyk, A.J. Dabrowski, NS-32 (1985) 533.

[148] G.R. Ricker, J.V. Vallerga, D.R. Wood, Nucl. Instr. and Meth. 213 (1983) 133.

[149] J.V. Vallerga, R.K. Vanderspek, G.R. Ricker, Nucl. Instr. and Meth. 213 (1983) 145.

[150] J.G. Bradley, J.M. Conley, A.L. Albee, J.S. Iwanczyk, A.J. Dabrowski, W.R. Warburton, Nucl. Instr. and Meth. A 283 (1989) 348.

[151] T. Economou, J. Iwanczyk, Nucl. Instr. and Meth. A 283 (1989) 352.

[152] R.B. James, J.F. Lathrop, S.J. Haney, D.J. Barry, D. Clark, T.R. Harrison, J. Harris, R.H. Stulen, Nucl. Instr. and Meth. A 294 (1990) 229.

[153] A. Friant, J. Mellet, G. Barrandon, E. Csakvary, Nucl. Instr. and Meth. A 283 (1989) 227.

[154] Y.J. Wang, J.S. Iwanczyk, W.R. Graham, IEEE Trans. Nucl. Sci. NS-40 (1993) 846.

[155] W. Autagawa, K. Zanio, J.W. Mayer, Nucl. Instr. and Meth. 55 (1967) 383.

[156] J.W. Mayer, J. Appl. Phys. 38 (1967) 296.

[157] V.S. Vavilov, R.Kh. Vagapov, V.A. Chapnin, M.V. Chukichev, Sov. Atomic Energy 28 (1970) 641.

[158] A. Cornet, P. Siffert, A. Coche, R. Triboulet, Appl. Phys. Lett. 17 (1970) 432.

[159] K. Zanio, J. Neeland, H. Montano, IEEE Trans. Nucl. Sci. NS-17 (1970) 287.

[160] R.C. Whited, M.M. Schieber, Nucl. Instr. and Meth. 162 (1979) 113.

[161] F.A. Kröger, D. de Nobel, J. Electron. 1 (1955) 190.

[162] D. de Nobel, Phillips Res. Rep. 14 (1959) 361.

[163] K. Zanio, Cadmium Telluride, Semiconductors and Semimetals, vol. 13, Academic Press, New York, 1978.

[164] M. Hage-Ali, P. Siffert, in T.E. Schlesinger, R.B. James, (Eds.), Semiconductors for Room Temperature Nuclear Detector Applications, Semiconductors and Semimetals, vol. 43, Academic Press, San Diego, 1995.

[165] M.R. Squillante, K.S. Shah, in: T.E. Schlesinger, R.B. James (Eds.), Semiconductors for Room Temperature Nuclear Detector Applications, Semiconductors and Semimetals, vol. 43, Academic Press, San Diego, 1995.

[166] R.O. Bell, F.V. Wald, IEEE Trans. Nucl. Sci. NS-19 (1972) 334.

[167] F.V. Wald, G. Entine, Nucl. Instr. and Meth. 150 (1978) 13.

[168] E. Raiskin, J.F. Butler, IEEE Trans. Nucl. Sci. NS-35 (1988) 81.

[169] M. Azoulay, A. Raizman, G. Gafni, M. Roth, J. Crystal Growth 101 (1990) 256.

[170] P. Rudolph, M. Mühlberg, Mat. Sci. Eng. B 16 (1993) 8.

[171] W.-M. Chang, W.R. Wilcox, L. Regel, Mat. Sci. Eng. B 16 (1993) 23.

[172] K. Zanio, F. Krajenbrink, H. Montano, IEEE Trans. Nucl. Sci. NS-21 (1974) 315.

[173] E.N. Arkad'eva, O.A. Mateev, E.V. Mel'nikova, A.I. Terent'ev, Sov. Phys. Semicond. 14 (1980) 839.

[174] M. Ohmori, Y. Iwase, R. Ohno, Nat. Sci. Eng. B 16 (1993) 283.

[175] T. Shoji, K. Ohba, H. Onabe, T. Suehiro, Y. Hiratate, IEEE Trans. Nucl. Sci. NS-40 (1993) 405.

[176] M. Hage-Ali, P. Siffert, Proc. MRS 299 (1994) 231.

[177] Ch. Steer, L. Chibani, J.M. Koebel, M. Hage-Ali, P. Siffert, Proc. MRS 299 (1994) 209.

[178] M. Hage-Ali, R. Stuck, C. Scharager, P. Siffert, IEEE Trans. Nucl. Sci. NS-26 (1979) 281.

[179] M. Hage-Ali, R. Stuck, A.N. Saxena, P. Siffert, Appl. Phys. 19 (1979) 25.

[180] S.L. Riedinger, D.W. Snyder, E.I. Ko, P.J. Sides, Mat. Sci. Eng. B 15 (1992) L9.

[181] S. Kohiki, K. Nishikura, T. Wada, T. Hirao, Appl. Surface Sci. 59 (1992) 39.

[182] S. Mergui, M. Hage-Ali, J.M. Koebel, P. Siffert, Nucl. Instr. and Meth. A 322 (1992) 375.

[183] A. Cornet, M. Hage-Ali, J.J. Grob, R. Stuck, P. Siffert, IEEE Trans. Nucl. Sci. NS-19 (1972) 358.

[184] M.R. Squillante, G. Entine, E. Frederick, L. Cirignano, T. Hazlett, Nucl. Instr. and Meth. A 283 (1989) 323.

[185] A. Kh. Khusainov, Nucl. Instr. and Meth. A 322 (1992) 335.

[186] S.H. Shin, G.T. Niizawa, J.G. Pasko, G.L. Bostrup, F.J. Ryan, M. Khoshenisan, C.I. Westmark, C. Fuller, IEEE Trans. Nucl. Sci. NS-32 (1985) 487.

[187] F.J. Ryan, S.H. Shin, D.D. Edwall, J.G. Pasko, M. Khoshnevisan, C.I. Westmark, C. Fuller, Appl. Phys. Lett. 46 (1985) 274.

[188] H.L. Malm, M. Martini, IEEE Trans. Nucl. Sci. NS-21 (1974) 322.

[189] P. Siffert, B. Rabin, H.Y. Tabatabai, R. Stuck, Nucl. Instr. and Meth. 150 (1978) 31.

[190] M. Hagi-Ali, M.C. Busch, J.M. Koebel, P. Siffert, Proc. SPIE 2305 (1994) 157.

[191] P. Siffert, J. Berger, C. Scharager, A. Cornet, R. Stuck, R.O. Bell, H.B. Serreze, F.V. Wald, IEEE Trans. Nucl. Sci. NS-23 (1976) 159.

[192] M. Hage-Ali, R. Stuck, C. Scharager, P. Siffert, IEEE Trans. Nucl. Sci. NS-26 (1979) 282.

[193] R.O. Bell, G. Entine, H.B. Serreze, Nucl. Instr. and Meth. 117 (1974) 267.

[194] W. Puschert, H. Scholtz, Appl. Phys. Lett. 28 (1976) 357.

[195] T. Taguchi, J. Shirafuji, Y. Inuishi, Nucl. Instr. and Meth. 150 (1978) 43.

[196] D. Vartsky, M. Goldberg, Y. Eisen, Y. Shamai, R. Dukhan, P. Siffert, J.M. Koebel, R. Regal, J. Gerber, Nucl. Instr. and Meth. A 263 (1988) 457.

[197] A.J. Dabrowski, J. Chwaszczewska, J. Iwanczyk, R. Triboulet, Y. Marfaing, IEEE Trans. Nucl. Sci. NS-23 (1976) 171.

[198] A.J. Dabrowski, J. Iwanczyk, W.M. Szymczyk, P. Kokoschinegg, J. Stelzhammer, R. Triboulet, Nucl. Instr. and Meth. 150 (1978) 25.

[199] V.F. Kushniruk et al., Sov. Atomic Phys. 42 (1977) 437.

[200] J. Pantazis, A. Huber, P. Okun, IEEE Trans. Nucl. Sci. NS-41 (1994) 1004.

[201] M.A. Lone, R.A. Leavitt, D.A. Harrison, Atomic Data and Nuclear Data Tables 26 (1981) 511.

[202] J.K. Tuli, in: Z.B. Alfassi, C. Chung (Eds.), Prompt Gamma Ray Activation Analysis, CRC Press, Boca Raton, FL, 1995, p. 177.

[203] A.G. Vradii, M.I. Krapivin, L.V. Maslova, O.A. Matveev, A. Kh. Khusainov, V.K. Shashurin, Sov. Atomic Energy 42 (1977) 64.

[204] P. Siffert, Proc. SPIE 2305 (1994) 98.

[205] R. Alt, P. Ambrosi, J. Böhm, G. Hilgers, M. Jordan, K.-H. Ritzenhoff, Nucl. Instr. and Meth. A 353 (1994) 71.

[206] L.T. Jones, P.B. Woollam, Nucl. Instr. and Meth. 124 (1975) 591.

[207] M.I. Krapivin, O.A. Matveev, A.G. Bradin, A. Kh. Khusainov, Sov. Atomic Energy 43 (1977) 633.

[208] M. Richter, P. Siffert, Nucl. Instr. and Meth. A 322 (1992) 529.

[209] M. Richter, P. Siffert, M. Hage-Ali, Mat. Sci. Eng. B 16 (1993) 296.

[210] Y. Eisen, Y. Horovitz, Nucl. Instr. and Meth. A 353 (1994) 60.

[211] Y. Takenaka, A. Uritani, K. Inoue, H. Sakai, O. Kubota, H. Toyokawa, C. Mori, Nucl. Instr. and Meth. A 369 (1996) 637.

[212] V.I. Ivanov, V.A. Garbusin, P.G. Dorogov, A.E. Loutchanski, V.V. Kondrashov, IEEE Trans. Nucl. Sci. NS-42 (1995) 258.

[213] G. Entine, D.A. Garcia, D.E. Tow, Rev. Phys. Appl. 12 (1977) 355.

[214] L. Kaufman, G. Gamsu, Ch. Savoca, S. Swann, Rev. Phys. Appl. 12 (1977) 369.

[215] J. Bojsen, N. Rossing, O. Soeberg, S. Vadstrup, Rev. Phys. Appl. 12 (1977) 361.

[216] J. Vogel, J. Ullman, G. Entine, Rev. Phys. Appl. 12 (1977) 375.

[217] J.L. Lazewatsky, N.M. Alpert, R.H. Moore, C.A. Boucher, H.W. Strauss, G. Entine, R. Chaney, R. Schreiner, IEEE Trans. Nucl. Sci. NS-27 (1980) 524.

IV. DETECTOR MATERIALS

[218] G. Entine, R.H. Redus, A. Feyder, P.J. Biggs, IEEE Trans. Nucl. Sci. NS-40 (1993) 1012.

[219] G. Entine, P. Waer, T. Tiernan, M.R. Squillante, Nucl. Instr. and Meth. A 283 (1989) 282.

[220] Y. Eisen, Nucl. Instr. and Meth. A 322 (1992) 596.

[221] C.R. Droms, W.R. Langdon, A.G. Robison, G. Entine, IEEE Trans. Nucl. Sci. NS-23 (1976) 498.

[222] L.T. Jones, Rev. Phys. Appl. 12 (1977) 379.

[223] M. Hage-Ali, J.M. Koebel, P. Siffert, V. Prat, H. Simon, Nucl. Instr. and Meth. A 369 (1996) 622.

[224] J.S. Gordon, S. Vasile, T. Hazlett, M. Squillante, IEEE Trans. Nucl. Sci. NS-40 (1993) 1162.

[225] R.J. Fox, D.C. Agouridis, Nucl. Instr. and Meth. 157 (1978) 65.

[226] M.A. Wolf, C.J. Umbarger, G. Entine, IEEE Trans. Nucl. Sci. NS-26 (1979) 777.

[227] G. Entine, R. Luthmann, W. Mauderli, L.T. Fitzgerald, C.M. Williams, C.H. Tosswill, IEEE Trans. Nucl. Sci. NS-26 (1979) 552.

[228] W. Dusi, E. Caroli, G. Di Cocco, A. Donati, G. Landini, J.B. Stephen, F. Casali, G. Baldazzi, P. Chirco, M. Rossi, Proc. SPIE 1734 (1992) 122.

[229] F. Casali, D. Bollini, P. Chirco, M. Rossi, G. Baldazzi, W. Dusi, E. Caroli, G. DiCocco, A. Donati, G. Landini, J.B. Stephen, IEEE Trans. Nucl. Sci. NS-39 (1992) 598.

[230] H. Tsutsui, T. Ohtsuchi, K. Ohmori, S. Baba, IEEE Trans. Nucl. Sci. NS-40 (1993) 40.

[231] H. Tsutsui, T. Ohtsuchi, K. Ohmori, S. Baba, IEEE Trans. Nucl. Sci. NS-40 (1993) 95.

[232] Y. Eisen, E. Polak, Proc. MRS, 299 (1994) 239.

[233] M. Merah, M. Riedinger, M. Hage-Ali, P. Siffert, Proc. SPIE 2305 (1994) 142.

[234] S.S. Yoo, S. Sivanathan, J.P. Faurie, B. Rodricks, J. Bai, P.A. Montano, Appl. Phys. Lett. 66 (1995) 2037.

[235] L.-A. Hamel, S. Paquet, Nucl. Instr. and Meth. A 380 (1996) 238.

[236] K. Guergouri, R. Triboulet, A. Tromson-Carli, Y. Marfaing, J. Crystal Growth 86 (1988) 61.

[237] M. Bruder, H.J. Schwartz, R. Schmitt, H. Maier, J. Crystal Growth 101 (1990) 266.

[238] F.P. Doty, J.F. Butler, J.F. Schetzina, K.A. Bowers, J. Vac. Sci. Technol. B 10 (1992) 1418.

[239] J.F. Butler, C.L. Lingren, F.P. Doty, IEEE Trans. Nucl. Sci. NS-39 (1992) 605.

[240] D.J. Olega, J.P. Faurie, S. Sivananthan, P.M. Raccah, Appl. Phys. Lett. 47 (1985) 1172.

[241] P. Capper (Ed.), Properties of Narrow Gap Cadmium-based Compounds, INSPEC, London, 1994.

[242] S.U. Egarievwe, L. Salary, K.T. Chen, A. Burger, R.B. James, Proc. SPIE 2305 (1994) 167.

[243] Z. Burshtein, H.N. Jayatirtha, A. Burger, J.F. Butler, B. Apotovsky, F.P. Doty, Appl. Phys. Lett. 63 (1993) 102.

[244] P. DeAntonis, E.J. Morton, F.J.W. Podd, IEEE Trans. Nucl. Sci. NS-43 (1996) 1487.

[245] J.F. Butler, F.P. Doty, C. Lingren, Proc. SPIE 1734 (1992) 131.

[246] J.F. Butler, F.P. Doty, B. Apotovsky, S.J. Friesenhahn, C. Lingren, Proc. MRS 302 (1993) 497.

[247] J.F. Butler, F.P. Doty, B. Apotovsky, J. Lajzerowicz, L. Verger, Mater. Sci. Eng. B 16 (1993) 291.

[248] F.P. Doty, S.J. Friesenhahn, J.F. Butler, P.L. Hink, Proc. SPIE 1945 (1993) 145.

[249] A. Parsons, C.M. Stahle, C.M. Lisse, S. Babu, N. Gehrels, B.J. Teegarden, P. Shu, Proc. SPIE 2305 (1994) 121.

[250] W.J. Hamilton, D.R. Rhiger, S. Sen, M.H. Kalisher, K. James, C.P. Reid, V. Gerrish, C.O. Baccash, IEEE Trans. Nucl. Sci. NS-41 (1994) 989.

[251] W.J. Hamilton, D.R. Rhiger, S. Sen, M.H. Kalisher, G.R. Chapman, R.E. Mills, J. Electron. Mater. 25 (1996) 1286.

[252] A. Niemelä, H. Sipilä, IEEE Trans. Nucl. Sci. NS-41 (1994) 1054.

[253] M.A. George, W.E. Collins, K.T. Chen, Z. Hu, S.U. Egarievwe, Y. Zheng, A. Burger, J. Appl. Phys. 77 (1995) 3134.

[254] H. Chen et al., Proc. SPIE 2859 (1996) 254.

[255] R. Hess, P. DeAntonis, E.J. Morton, W.B. Gilboy, Nucl. Instr. and Meth. A 353 (1994) 76.

[256] R.B. James, T.E. Schlesinger, J. Lund, M. Schieber, in: T.E. Schlesinger, R.B. James (Eds.), Semiconductors for Room Temperature Nuclear Detector Applications, Semiconductors and Semimetals, vol. 43, Academic Press, San Diego, 1995.

[257] J.C. Lund, R. Olsen, J.M. van Scyoc, R.B. James, IEEE Trans. Nucl. Sci. NS-43 (1996) 1411.

[258] A. Niemelä, H. Sipilä, V.I. Ivanov, IEEE Trans. Nucl. Sci. NS-43 (1996) 1476.

[259] P.N. Luke, Appl. Phys. Lett. 65 (1994) 2884.

[260] P.N. Luke, IEEE Trans. Nucl. Sci. NS-42 (1995) 207.

[261] Z. He, Nucl. Instr. and Meth. A 365 (1995) 572.

[262] P.N. Luke, E.E. Eissler, IEEE Trans. Nucl. Sci. 43 (1996) 1481.

[263] Z. He et al., Nucl. Instr. and Meth. A 380 (1996) 228.

[264] O. Frisch, British Atomic Energy Report, BR-49, 1944.

[265] Z. He, G.F. Knoll, D.K. Wehe, J. Miyamoto, IEEE Trans. Nucl. Sci. (1997), in press.

[266] R. Olsen, R.B. James, A.J. Antolak, C. Wang, Proc. Nucl. Mater. Management 23 (1994) 589.

[267] D.S. McGregor, J.T. Lindsay, R.W. Olsen, Nucl. Instr. and Meth. A 381 (1996) 498.

[268] L.M. Bartlett et al., Proc. SPIE 2859 (1996) 10.

[269] M.R. Daily et al., Proc. Nucl. Mater. Management 24 (1995) 597.

[270] R. Olsen, J. Lund, R. Miller, R. James, A. Antolak, M. Daily, Proc. Nucl. Mater. Management, 24 (1995) 593.

[271] R.W. Olsen, R.B. James, C. Cofield, B. Miller, B. Mickelsen, Nucl. Instr. and Meth. A 380 (1996) 467.

[272] W.D. Ruhter, R. Gunnink, Nucl. Instr. and Meth. A 353 (1994) 716.

[273] R. Polichar, R. Schirato, J. Reed, Proc. SPIE 1736 (1992) 43.

[274] J.F. Butler, S.J. Friesenhahn, C. Lingren, B. Apotovasky, F.P. Doty, W.L. Ashburn, W. Dillon, Proc. SPIE 1896 (1993) 30.

[275] R. Polichar, R. Schirato, J. Reed, Nucl. Instr. and Meth. A 353 (1994) 349.

[276] F.P. Doty, H.B. Barber, F.L. Augustine, J.F. Butler, B.A. Apotovsky, E.T. Young, W. Hamilton, Nucl. Instr. and Meth. A 353 (1994) 356.

[277] G. Baldazzi et al., IEEE Trans. Nucl. Sci. NS-42 (1995) 575.

[278] L.A. Hamel, J.R. Macri, C.M. Stahle, J. Odom, F. Birsa, P. Shu, F.P. Doty, IEEE Trans. Nucl. Sci. NS-43 (1996) 1422.

[279] T.O. Tümer et al., IEEE Trans. Nucl. Sci. NS-43 (1996) 1417.

[280] J.R. Macri et al., IEEE Trans. Nucl. Sci. NS-43 (1996) 1458.

[281] D.G. Marks et al., IEEE Trans. Nucl. Sci. NS-43 (1996) 1253.

[282] S. Roth, W.R. Willig, Appl. Phys. Lett. 18 (1971) 328.

[283] W.R. Willig, Nucl. Instr. and Meth. 101 (1972) 23.

[284] C. Manfredotti, R. Murri, A. Quirini, L. Vasanelli, IEEE Trans. Nucl. Sci. NS-24 (1977) 126.

[285] J.C. Lund, K.S. Shah, M.R. Squillante, F. Sinclair, IEEE Trans. Nucl. Sci. NS-35 (1988) 89.

[286] L.C. Lund, K.S. Shah, M.R. Squillante, L.P. Moy, F. Sinclair, G. Entine, Nucl. Instr. and Meth. A 283 (1989) 299.

[287] J.C. Lund, K.S. Shah, F. Olschner, J. Zhang, L. Moy, S. Medrick, M.R. Squillante A 322 (1992) 464.

[288] D.C. David, A. Burger, W. Wang, R.B. James, T.E. Schlesinger, J.C. Lund, Proc. SPIE 1734 (1992) 146.

[289] K.S. Shah, J.C. Lund, F. Olschner, P. Bennett, J. Zhang, L.P. Moy, M.R. Squillante, Nucl. Instr. and Meth. A 353 (1994) 85.

[290] T. Shoji, K. Ohba, T. Suehiro, Y. Hiratate, IEEE Trans. Nucl. Sci. NS-42 (1995) 659.

[291] V. Deich, M. Roth, Nucl. Instr. and Meth. A 380 (1996) 169.

[292] A.E. Dugan, H.K. Henisch, J. Phys. Chem. Solids 28 (1967) 1885.

[293] T. Yao, I. Imai, Solid State Commun. 9 (1971) 205.

[294] J.C. Lund, F. Olschner, A. Burger, in: T.E. Schlesinger, R.B. James (Eds.), Semiconductors for Room Temperature Nuclear Detector Applications, Semiconductors and Semimetals, vol. 43, Academic Press, San Diego, 1995.

[295] J.C. Lund, F. Olschner, F. Sinclair, M.R. Squillante, Nucl. Instr. and Meth. A 272 (1988) 885.

[296] F. Olschner, J.C. Lund, M.R. Squillante, D.L. Kelly, IEEE Trans. Nucl. Sci. NS-36 (1989) 210.

[297] Y. Suzuki, Y. Fukuda, Y. Nagashima, H. Kan, Nucl. Instr. and Meth. A 275 (1989) 142.

[298] A. Valentini, A. Cola, G. Maggi, V. Paticchio, F. Quaranta, L. Vasanelli, Nucl. Instr. and Meth. A 373 (1996) 47.

[299] W. Shockley, Solid State Electron. 2 (1961) 35.

[300] C.A. Klein, IEEE Trans. Nucl. Sci. NS-15 (1968) 214.

[301] R. Raghavan, Phys. Rev. Lett. 37 (1976) 259.

[302] R.B. Hammond, N.G. Paulter, A.E. Iverson, R.C. Smith, IEDM Tech. Digest, Washington, DC, 1981, p. 157.

[303] A.G. Foyt, F.J. Leonberger, R.C. Williamson, Appl. Phys. Lett. 40 (1982) 448.

[304] T.F. Deutsch, F.J. Leonberger, A.G. Foyt, D. Mills, Appl. Phys. Lett. 41 (1982) 403.

[305] R.B. Hammond, N.G. Paulter, R.S. Wagner, T.E. Springer, M.D.J. MacRoberts, IEEE Trans. Elec. Dev. ED-30 (1983) 412.

[306] R.B. Hammond, N.G. Paulter, R.S. Wagner, T.E. Springer, Appl. Phys. Lett. 44 (1984) 620.

[307] D.R. Kania, R.J. Bartlett, R.S. Wagner, R.B. Hammond, P. Pianetta, Nucl. Instr. and Meth. 222 (1984) 270.

[308] D.R. Kania, R.J. Bartlett, R.S. Wagner, R.B. Hammond, P. Pianetta, Appl. Phys. Lett. 44 (1984) 1059.

[309] D.R. Kania, A.E. Iverson, D.L. Smith, R.S. Wagner, R.B. Hammond, K.A. Stetler, J. Appl. Phys. 60 (1986) 2596.

[310] A. Burger, I. Shilo, M. Schieber, IEEE Trans. Nucl. Sci. NS-30 (1983) 368.

[311] A. Burger, M. Roth, J. Crystal Growth 67 (1984) 507.

[312] M. Roth, A. Burger, IEEE Trans. Nucl. Sci. NS-33 (1986) 407.

[313] M. Roth, A. Burger, J. Nissenbaum, M. Schieber, IEEE Trans. Nucl. Sci. NS-34 (1987) 465.

[314] M. Roth, Nucl. Instr. and Meth. A 283 (1989) 291.

[315] C. Canali, F. Nava, G. Ottaviani, C. Paorici, Solid State Commun. 11 (1972) 105.

[316] A. Burger, M. Roth, J. Crystal Growth 70 (1984) 386.

[317] A. Burger, M. Roth, M. Schieber, IEEE Trans. Nucl. Sci. NS-32 (1985) 556.

[318] C. Manfredotti, R. Murri, L. Vasanelli, Nucl. Instr. and Meth. 115 (1974) 349.

[319] C. Manfredotti, R. Murri, A. Quirini, L. Vasanelli, Nucl. Instr. and Meth. 131 (1975) 457.

[320] A.M. Mancini, C. Manfredotti, R. Murri, A. Rizzo, A. Quirini, L. Vasanelli, IEEE Trans. Nucl. Sci. NS-23 (1976) 189.

[321] E. Sakai, H. Nakatani, C. Tatsuyama, F. Takeda, IEEE Trans. Nucl. Sci. NS-35 (1988) 85.

[322] H. Nakatani, E. Sakai, C. Tatsuyama, F. Takeda, Nucl. Instr. and Meth. A 283 (1989) 303.

[323] T. Yamazaki, H. Nakatani, N. Ikeda, Jpn. J. Appl. Phys. 32 (1993) 1857.

[324] V.M. Arutyunyan, M.L. Dimaksyan, V.L. Elbakyan, G.E. Grigoryan, Sov. Phys. Semicond. 23 (1989) 315.

[325] I. Rahman, R. Hofstadter, Phys. Rev. B 29 (1984) 3500.

[326] I. Rahman, W.A. Fisher, R. Hofstadter, S. Jing, Nucl. Instr. and Meth. A 261 (1987) 427.

[327] K.S. Shah, J.C. Lund, F. Olschner, L. Moy, M.R. Squillante, IEEE Trans. Nucl. Sci. NS-36 (1989) 199.

[328] F. Olschner, M. Toledo-Quinones, K.S. Shah, J.C. Lund, IEEE Trans. Nucl. Sci. NS-37 (1990) 1162.

[329] K.S. Shah, F. Olschner, L.P. Moy, J.C. Lund, M.R. Squillante, Nucl. Instr. and Meth. A 299 (1990) 57.

[330] K.S. Shah, J.C. Lund, F. Olschner, J. Zhang, L.P. Moy, M.R. Squillante, W.W. Moses, S.E. Derenzo, IEEE Trans. Nucl. Sci. NS-41 (1994) 2715.

[331] Y. Kumashiro, J. Mater. Res. 5 (1990) 2833.

[332] B. Stone, D. Hill, Phys. Rev. Lett. 4 (1960) 282.

[333] R.J. Archer, R.Y. Koyama, E.E. Loebner, R.C. Lucas, Phys. Rev. Lett. 12 (1964) 538.

[334] Y. Kumashiro, K. Kudo, K. Matsumoto, Y. Okada, T. Koshiro, J. Less-Common Metals 143 (1988) 71.

[335] T.L. Chu, J.M. Jackson, A.E. Hyslop, S.C. Chu, J. Appl. Phys. 42 (1971) 420.

[336] J.L. Peret, J. Am. Ceramic Soc. 47 (1964) 44.

[337] T.L. Chu, J.M. Jackson, S.K. Smeltzer, J. Crystal Growth 15 (1972) 254.

[338] Y. Kumashiro, T. Yao, S. Gonda, J. Crystal Growth 70 (1984) 515.

[339] Y. Kumashiro, T. Yao, S. Gonda, J. Crystal Growth 70 (1984) 507.

IV. DETECTOR MATERIALS

[340] Y. Kumashiro, Y. Okada, S. Misawa, T. Koshiro, Proc. 10th Int. Conf. Chemical Vapor Deposition, vol. 87-8, 1987, p. 813.

[341] Y. Kumashiro, Y. Okada, Appl. Phys. Lett. 47 (1985) 64.

[342] J. Electrochem. Soc. 136 (1989) 1830.

[343] J.H. Yee, S.P. Swierkowski, J.W. Sherohman, IEEE Trans. Nucl. Sci. NS-24 (1977) 1962.

[344] R. Linnebach, K.W. Benz, J. Crystal Growth 53 (1981) 579.

[345] K.B. McAfee, Jr., D.M. Gay, R.S. Hozack, R.A. Laudise, W.A. Sunder, J. Crystal Growth 88 (1988) 488.

[346] C.T. Lin, E. Schönherr, H. Bender, C. Busch, J. Crystal Growth 94 (1989) 955.

[347] R.T. Johnson, Jr., J. Appl. Phys. 41 (1970) 4981.

[348] T.M. Bochkova, A.V. Kovalenko, Nucl. Tracks Radiat. Meas. 21 (1993) 191.

[349] E.E. Eissler, K.G. Lynn, IEEE Trans. Nucl. Sci. NS-42 (1995) 663.

[350] K.S. Shah, L.P. Moy, J. Zhang, S. Medrick, F. Olschner, M.R. Squillante, Proc. SPIE 1734 (1992) 161.

[351] M.R. Squillante, C. Zhou, J. Zhang, L.P. Moy, K.S. Shah, IEEE Trans. Nucl. Sci. NS-40 (1993) 364.

[352] B. Goldstein, J. Appl. Phys. 36 (1965) 3853.

[353] P.C. Canepa, P. Malinaric, R.B. Campbell, J. Ostroski, IEEE Trans. Nucl. Sci. NS-11 (1964) 262.

[354] M.B. Prince, P. Polishuk, IEEE Trans. Nucl. Sci. NS-14 (1967) 537.